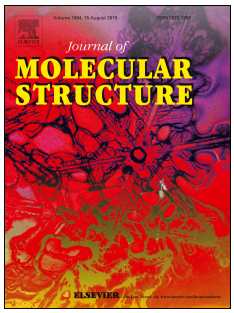

New complexes of manganese (II) and copper (II) derived from the two new furopyran-3, 4-dione ligands: Synthesis, spectral characterization, ESR, DFT studies and evaluation of antimicrobial activity

Yamina Abdi, Nadjia Bensouilah, Dhaouya Siziani, Maamar Hamdi, Artur M.S. Silva, Baya Boutemeur-Kheddis

PII: S0022-2860(19)31416-4

DOI: https://doi.org/10.1016/j.molstruc.2019.127307

Reference: MOLSTR 127307

To appear in: *Journal of Molecular Structure*

Received Date: 26 March 2019

Revised Date: 20 September 2019

Accepted Date: 27 October 2019

Please cite this article as: Y. Abdi, N. Bensouilah, D. Siziani, M. Hamdi, A.M.S. Silva, B. Boutemeur-Kheddis, New complexes of manganese (II) and copper (II) derived from the two new furopyran-3, 4-dione ligands: Synthesis, spectral characterization, ESR, DFT studies and evaluation of antimicrobial activity, *Journal of Molecular Structure* (2019), doi: https://doi.org/10.1016/j.molstruc.2019.127307.

New complexes of manganese (II) and copper (II) derived from the two new Furopyran-3, 4-dione ligands: Synthesis, spectral characterization, ESR, DFT studies and evaluation of antimicrobial activity

Yamina Abdi[a,b] , Nadjia Bensouilah[a*], Dhaouya Siziani[a,c], Maamar Hamdi[a], Artur M. S. Silva[d] , Baya Boutemeur-Kheddis[a]

[a] *Laboratoire de Chimie Organique Appliquée (Groupe Hétérocycles), Faculté de Chimie, Université des Sciences et de la Technologie Houari Boumediène BP 32, El-Alia Bab-Ezzouar, 16111, Algiers, Algeria*
[b]*Ecole Nationale Supérieure de Technologie Cité Diplomatique Ex Centre Biomédical Dergana-Bordj El Kiffan-, Algiers, Algeria*
[c]*Ecole Supérieure des Sciences Appliquées d'Alger, BP 474, Place des Martyrs, Alger 16001, 1er Novembre, Algiers, Algeria.*
[d]*QOPNA, Department of Chemistry, University of Aveiro, 3810-193 Aveiro, Portugal*

Abstract:

A total of four new metal complex derivatives of two new ligands 2-(hydroxy(phenyl)-6-methyl-2H-furo[3,2-c]pyran-3,4-dione (**L^1**) and 2-(hydroxyl (2-hydroxyphenyl) -6-methyl-2H-furo[3,2-c]pyran-3,4-dione (**L^2**) with the metal ions Mn(II) and Cu(II) have been successfully prepared in alcoholic medium. The complexes obtained are investigated by spectral studies with the use of FT-IR and UV-vis techniques, ESR and magnetic measurements. The IR spectra suggest that the oxygen atoms of the two ligands are engaged in the bond with the central metal. The electronic spectra of the complexes and their magnetic moments provide information about geometries. The molar conductance measurements showed that the complexes are non-electrolytes. Theoretical calculations invoking geometry optimization and molecular orbital description HOMO and LUMO are done using DFT density functional theory. The experimental results and the calculated structural parameters, bond distances and angles, revealed a distorted octahedral geometries around the manganese and copper center through the oxygen of the furan ring for the synthesized complexes ($[M(L)_2(H_2O)_2]nH_2O$; M : metal; L: ligand). The antimicrobial activity of the ligands and their complexes was evaluated in vitro against different bacteria and fungi using agar diffusion method. The ligands and their complexes of manganese (II) and copper (II) exhibited a strong antifungal activity. Copper and manganese complexes have different antibacterial properties against bacteria. The ligand L^1 and there complexes were found to be more active against Gram-positive than Gram-negative bacteria.

Keywords: Heterocyclic ligands; ligand derived from the furopyran-3,4-dione; Metal complexes; ESR; DFT, Antimicrobial activity.

1. Introduction:

In recent years, the coordination chemistry of copper (II) with oxygenated and nitrogenous heterocyclic compounds has attracted considerable interest. This can be attributed to their stability, biological activity and potential applications in many areas [1, 2]. Manganese is one of the most important biometals, it is found in the active center of many enzymes covering the whole range of functionalities [3]. The study of the biological properties of manganese complexes gains increasing interest since such complexes with diverse ligands have shown anticancer [4], antibacterial [5] and antifungal [6] activities.

The oxygen containing hetrocyclic compounds especially the pyrones and their derivatives were used for the preparation of transition metal complexes with hetrocyclic system are studied extensively because of their biological activities. Pyran-2-ones and furan-3-ones are important oxygen heterocycles which are mostly present in the structure of a variety of biologically active natural compounds [7-10]. Among organic compounds, which can serve as ligands, 2-pyrone ring and its derivatives have received much interest because of their many interesting features [11]. They demonstrate a whole spectrum of bioactivity and have shown antibiotic, antifungal, cytotoxic, neurotoxic, and phytotoxic activities. Simple functionalization of the 2-pyrone ring often leads to compounds with new biological activity [12-14]. Furan-3-one-containing molecules continue to attract interest, and they have recently reported some valuable anticancer template [15–16].

The different complexes with different types of drugs heterocyclic such as imines, amines, imidazole groups and ligands containing 2-pyrone ring play an important role in biology and medicine areas [17]. These ligands are often used in medicine, for their pharmacological properties such as antibacterial activity [18–21]. The metal complexes with 2-pyrone derivatives are topic of increasing interest in the bioinorganic and coordination chemistry [22–26]. Indeed, we are interested in furopyran-3, 4-dione and its derivatives because of their pharmaceutical and chemical importance. They form coordination complexes with transition metal ion like Cu (II) and Mn (II). The literature survey show that there is no work found to be done on furopyran-3, 4-diones metal chelate complexes. Therefore, we are involved in the coordination complexes of furopyran-3, 4-diones with transition metal ions like Cu (II) and Mn (II) ions.

On the basis of previous works and more particularly coordination complexes [27-31], we have synthesized and characterized manganese (II) and copper (II) complexes obtained from furopyran-3,4-diones derivatives as ligands.

All synthesized complexes have been satisfactorily characterized by elemental analysis, magnetic susceptibility measurements in the solid state and various spectroscopic techniques such as: FT-IR, UV-vis. The theoretical results obtained with the DFT calculations have been correlated with experimental data to confirm the proposed coordination mode in the copper and manganese complexes. At the end of our work, the antimicrobial activity of the new manganese and copper complexes formed with derived furopyran-3, 4-dione ligands was experimentally explored to evaluate their antibacterial and the antifungal susceptibilities.

2. Experimental:

2.1 Synthesis of ligands:

We have recently published synthesis and structure of Novel furopyran-3, 4-dione-fused heterocycles obtained by a one-pot reaction of α-brominated dehydroacetic acid and benzaldehydes under organobase conditions. The prepared 2-[aryl (hydroxy) methyl]-6-methyl-2H-furo[3,2-c]pyran-3,4-diones were fully characterized by 2D NMR spectroscopy and supported by single crystal X-ray analysis to prove the furan-3-one five-membered ring-closure [32].

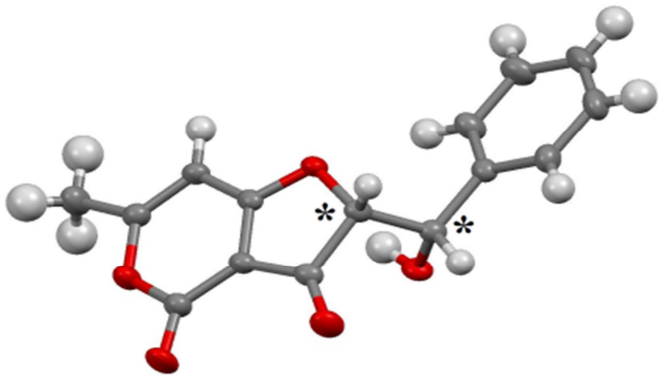

Fig.1. Schematic representation of the molecular unit present in the asymmetric unit of ligand L^1.

Single-crystal X-ray diffraction was performed in order to describe the 3D structure of the furopyran-3, 4-dione **L^1**. Good quality crystals of compound **L^1** were isolated from a 5:2 mixture of hexane–ethanol by a slow evaporation at 6 °C. X-ray diffraction analysis revealed the exact structure of **L^1**, which is in a complete agreement with the 2D NMR results [32]. Two asymmetric carbon atoms (C_8 and C_9 crystallographic numbering, see Figure 1) are clearly observed in the crystal structure. Because **L^1** crystallizes in

centrosymmetric P1 triclinic space groups, the unit cell contains the mirror image of the organic molecule depicted in Figure 1, leading to a solid-state racemic mixture of two possible enantiomers [(2R,1′S) and (2S,1′R)]. Two products were selected as ligands (L^1 and L^2) in the synthesis of a new Cu (II) and Mn (II) complexes (see figure 2).

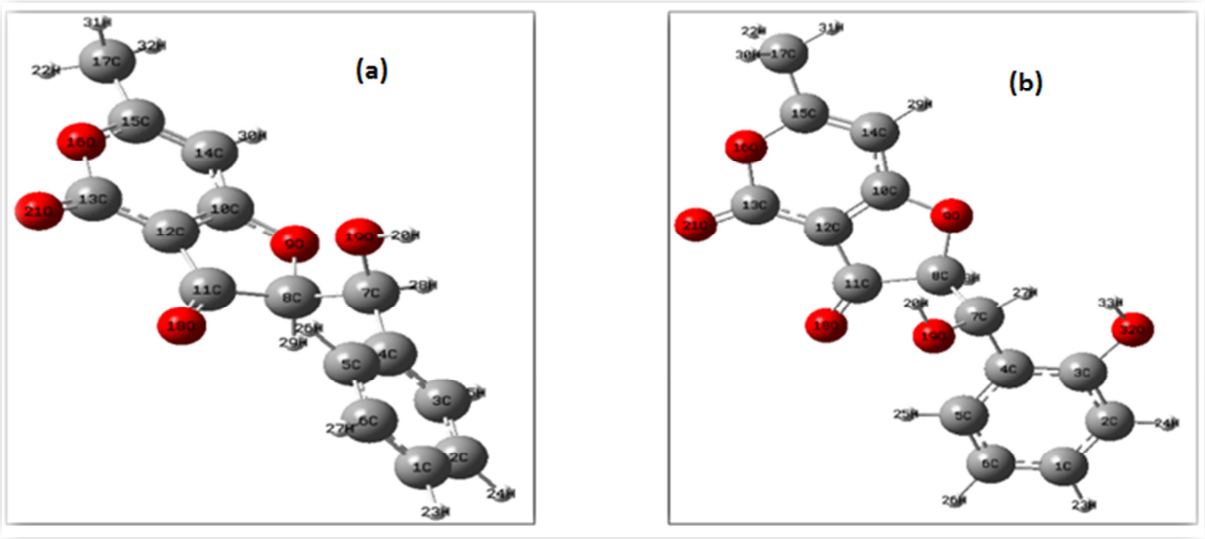

Fig.2. Structure of derived Furopyran-3, 4-dione ligands; **(a)** $\mathbf{L^1}$: 2-(hydroxy(phenyl)-6-methyl-2H-furo[3,2-c]pyran-3,4-dione and **(b)** $\mathbf{L^2}$: 2-(hydroxy(2-hydroxyphenyl)-6-methyl-2H-furo[3,2-c]pyran-3,4-dione optimized with DFT method.

2.2 Synthesis of complexes:

The starting materials for the synthesis of organometallic complexes were purchased from Fluka and Aldrich and were used without purification. The used salts are of the type of : $MnCl_2.4H_2O$ and $CuCl_2.2H_2O$.

- ***[Mn(L^1)$_2$(H_2O)$_2$]H_2O and [Mn(L^2)$_2$(H_2O)$_2$]2H_2O:***

A solution of $MnCl_2.4H_2O$ (1mmol) in ethanol (6 ml) was added drop wise to a solution of ligand (2mmol) in a hot ethanol (10 ml) in a 1:2 metal to ligand molar ratio. The resulting mixture was heated under reflux for about 16 h. The obtained complexes were washed with distilled water and ethanol, dried at 60 °C and finally stored in vacuum desiccators.

- ***[Cu(L^1)$_2$ (H_2O)$_2$].H_2O and [Cu(L^2)$_2$ (H_2O)$_2$]2H_2O:***

A solution of $CuCl_2.2H_2O$ (1mmol) in ethanol (6 ml) was added dropwise to a solution of ligand (2 mmol) in a hot ethanol (10 ml) in a 1:2 metal to ligand molar ratio. The resulting mixture was heated under reflux over 8 h. The obtained complexes were washed with distiller water and ethanol, dried at 60 °C and finally stored in vacuum desiccators.

2.3 *Apparatus and characterizations:*

Elemental analyses were carried out using a Perkin–Elmer Analyser 2400. The melting points were determined with a digital melting points apparatus using capillary technique. The molar conductance measurements of the compounds (10^{-3} M) were carried out using a JENWAY-4520 conductometer at 25 °C from 10^{-3} M solution in DMSO (Molar conductance of DMSO = 0.41 Ω^{-1} cm^2 mol^{-1}). IR spectra were recorded on Perkin Elmer FT-IR Fourier transform infrared spectrometer, in the range 4000-400 cm^{-1}, using KBr disks. Electronic absorption spectra in DMSO solutions (10^{-3} and 10^{-4}M) were recorded on an UV-Visible JASCO V-560 spectrophotometer using quartz cells (0.5 cm) in the 900-200 nm range. The ESR measurements were performed in solution at 115 K and in solid state at room temperature, on a Bruker EMX spectrophotometer. The magnetic measurements were carried out using SQUID magnetometer in 200-300 K range with an applied field 10,000G.

3. Theoretical calculations:

Quantum Chemical calculations were performed with GAUSSIAN 03 program packaged [33]. The geometry of the complexes was optimized using Density Functional Theory (DFT). All theoretical calculations were carried out at gradient corrected DFT using Becke's three parameter hybrid method and the Lee–Yang–Parr correlation functional B3LYP [34-36] combined with LANL2DZ basis set [37-38]. The studied forms of complexes were characterized as minima (no negative eigenvalues) in their potential energy surface through harmonic frequency analysis and their vibration spectra were analyzed using Gauss view software [39]. The oscillation strengths (*f*), wavelengths (λ_{max}) and Solvent effect on absorption UV-vis spectrum were investigated using the TD-DFT on the fully DFT optimized geometries. The continuum model (CPCM) was chosen in these calculations.

4. Antimicrobial Activity of complexes (in vitro):

Microorganisms and culture conditions:

The antimicrobial activities were tested against standard strains of Gram-negative bacteria *(Escherichia coli* ATCC 4157, *Klebsiella pneumoniae* ATCC 25955) and Gram-positive bacteria (*Staphylococcus aureus* ATCC 6538, *Group D Streptococcus* ATCC

25923), and two yeasts (*Candida albicans* ATCC 24433, *Candida tropicalis* ATCC 10233). The antimicrobial activity of ligands and their complexes was determined by agar disc diffusion method [40-42]. The molten Mueller Hinton Agar for bacteria and Sabouraud dextrose agar media for fungi was inoculated with **100 µL** of the inoculum (10^6 CFU/mL) at 40°C and then poured into the Petri plate (90 mm). Sterile disc (9 mm: 710 0223, VWR) was saturated with 25 µL of the test compound with the concentration 5 mg/mL in DMSO and allowed to dry. The disc was then introduced on the layer of the seeded agar plate. For each microbial strain, negative controls were maintained and a negative effect was observed with DMSO solvent. The bacterial and fungal plates were incubated at 37°C for 24 h and at 28 °C for 48 h, respectively. Gentamicine (GEN) and Cefotaxime (CTX) were used as a standard reference in the case of bacteria while ketoconazole were used as a standard antifungal [43]. The antimicrobial activity was determined by measuring the diameter of inhibition zones and the values were compared with the standard antimicrobials.

5. Results and discussion:

5.1 *Analytical and physical data of the complexes:*

The analytical data and physical properties of the complexes are summarized in Table 1. The synthesized complexes are totally soluble in DMSO and DMF, partially soluble in ethanol and methanol. Their molar conductance data in 10^{-3}M DMSO solution at 25 °C revealed that they are non electrolyte species [44]. The magnetic measurements for manganese complexes fall in the 4.71–4.88 B.M. range, suggesting a high spin Mn (II) in an octahedral geometry [49,52] (Table 1). The observed magnetic moment in the 1.88–2.01 B.M. range confirms mononuclear Cu (II) compounds with a s=1/2 spin state and an octahedral structure [50,56–57,45] (see Table 1).

Thus, the elemental analyses along with magnetic moment measurements suggest octahedral complexes. In addition, confirmation of the proposed structures of the chelates with metal salt was done using other experimental characterization methods namely: UV-vis, FT-IR and ESR data. The corresponding spectroscopic results will be detailed in the spectral sections (see 5.3, 5.4, and 5.5 parts)

Table 1: Analytical and physical data of the complexes.

Complexes	Exp (Cal)(%) C	H	O	M*	Melting point °C	Color	Yield (%)	Λ_{DMSO} ($\Omega^{-1}.cm^2.mol^{-1}$)	μ_{eff} (M.B)
$[Mn(L^1)_2(H_2O)_2].H_2O$	55.89 (55.34)	4.54 (4.30)	31.49 (31.95)	8.51 (8.44)	256	Brown	51	22	4.71
$[Mn(L^2)_2(H_2O)_2].H_2O$	52.47 (52.71)	4.54 (4.10)	35.37 (35.14)	8.62 (8.04)	263	Brown	63	25	4.88
$[Cu(L^1)_2(H_2O)_2].H_2O$	53.58 (53.13)	4.73 (4.43)	33.46 (33.06)	9.81 (9.38)	> 300	Green	58	17	1.88
$[Cu(L^2)_2(H_2O)_2].H_2O$	52.35 (52.06)	4.48 (4.05)	34.13 (34.70)	8.86 (9.18)	> 300	Green	51	21	2.01

* Metal: Manganese Mn or Copper Cu.

5.2 Geometry optimization:

On the basis of the Analytical and physical results of these complexes, we suggest that the ligands are coordinated in a deprotonated form leading to octahedral complexes (neutral complexes). Selected bond distances, angles and dihedral angles for the four complexes are listed in Table S1 (in supplementary data SI). Indeed, according to the DFT study, the Cu(II) and Mn (II) adopt a distorted octahedral geometry, where L^1 and L^2 act as a bidentate ligand through both the carbonyl oxygen and charged oxygen [Mn63O18 = 2.21Å and Mn63O19 = 2.11 Å and Mn63O49 = 2.26Å and Mn63O50 = 2.098 Å for [$MnL^1(H_2O)_2].H_2O$ complex]; See figure 3. The ligands form a square planar arrangement of above donor groups around the manganese ion. The two other axial sites are occupied by water molecules.

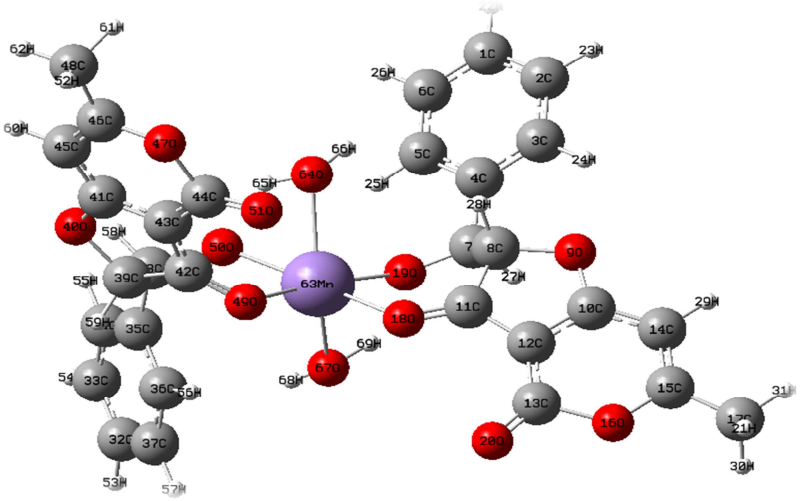

Fig.3. Structure of $[Mn(L^1)_2.(H_2O)_2].H_2O$ complex optimized at DFT method

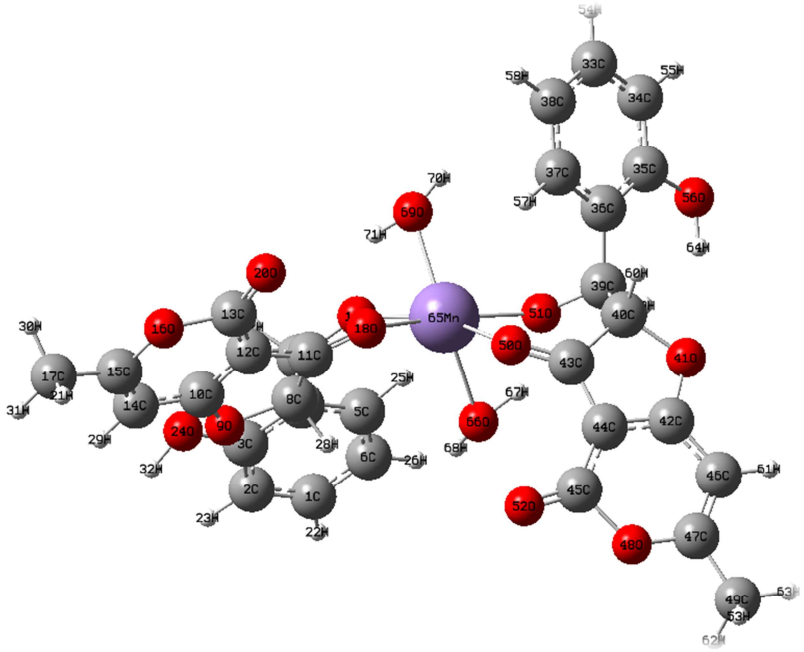

Fig.4. Structure of $[Mn(L^2)_2.(H_2O)_2].H_2O$ complex optimized at DFT method.

It is worthy of note that in $[Mn(L^1)_2.(H_2O)_2].H_2O$ complex, the Mn63…O50 and Mn63…O19 bond lengths (in the charged Oxygen site) are shorter than the Mn63…O49 and Mn…O18 bond lengths (in carbonyl moiety) indicating that the coordination ability in deprotonated site of hydroxyl group is stronger than that of carbonyl oxygen of both ligands. Similarly for the $[Mn(L^2)_2.(H_2O)_2].H_2O$ complex, the Mn65…O51 and Mn65…O19 bond lengths (in the charged Oxygen site) are shorter than the Mn65…O50 and Mn…O18 bond lengths. (See the corresponding values in SI). It is also noticed from the DFT data, that the distance of Mn63-O50 in first ligand $L^1$is shorter than that L^2 ligand (Mn65-O19) in deprotonated site. Hence, the coordination ability of Mn ion of $[Mn(L^1)_2\ (H_2O)_2].H_2O$ is

slightly stronger than that of Mn ion of $[Mn(L^2)_2\ (H_2O)_2].H_2O$. In $[Mn(L^1)_2\ (H_2O)_2].H_2O$ complex, two aqua ($O64H_2$ and $O67H_2$) molecules are lying in the molecular plane in trans position with a bond angle of 147.85° (see fig. 1). Two aqua ($O66H_2$ and $O69H_2$) molecules are also lying in molecular plan in $[Mn(L^2)_2\ (H_2O)_2].H_2O$ complex with a bond of 147.039° (see fig.4). The O64Mn63O67 and O66Mn65O69 angles deviate from linearity (180) indicating a distortion in the basal plane.

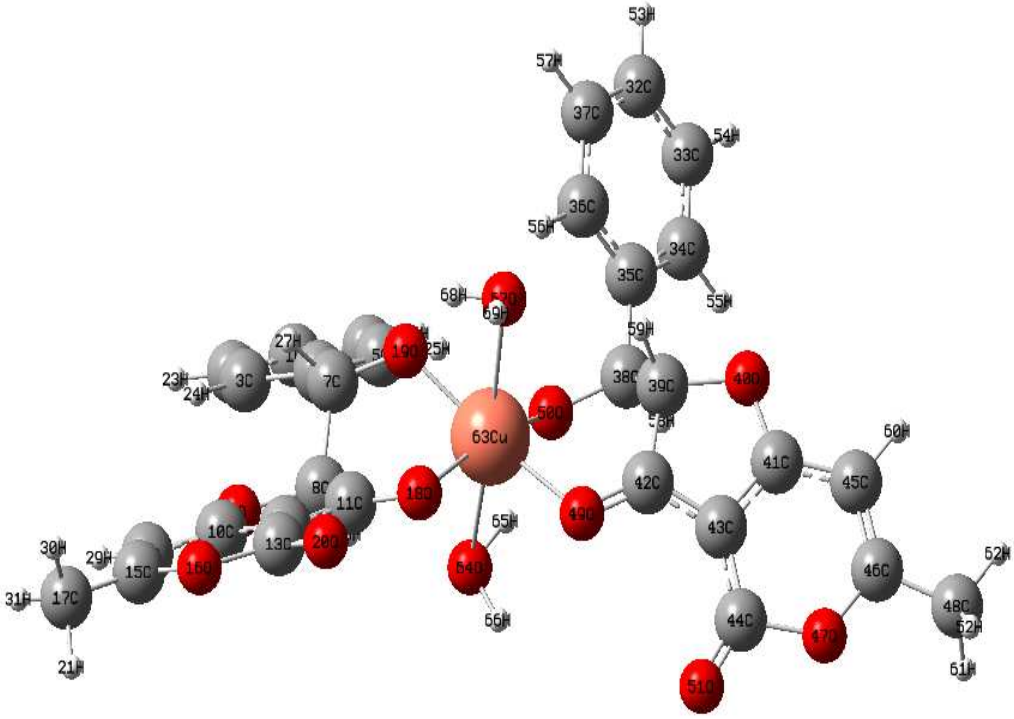

Fig.5. Structure of $[Cu(L^1)_2(H_2O)_2].H_2O$ optimized at DFT method

The same general situation was observed for the copper complexes with above ligands. It is important to note that, in both copper complexes, the Cu…O coordination bond lengths for deprotonated oxygen are also shorter than those of the carbonyl oxygen. In parallel, the bond lengths of Cu…O (hydrated) are more important comparing to those of manganese complexes and the linearity with aqua molecules and the metallic central is more pronounced, this result is justified by the following values of corresponding angles : O64-Cu63-O67 (174.209°) and O62-Cu61-O65 (171.978°) for $[Cu(L^1)_2(H_2O)_2].H_2O$ complex and $[Cu(L^2)_2(H_2O)_2].H_2O$ complex respectively (see figs. 5,6).

The corresponding calculated structural parameters are dressed in the same table in supplementary information SI. Subsequently, we calculated the binding energies of the

four complexes. We followed the same procedure described in the references [45-47]. Thus, the corresponding values of the $Mn(L^1)_2(H_2O)_2$, $Mn(L^2)_2(H_2O)_2$, $Cu(L^1)2(H_2O)_2$, $Cu(L^2)_2(H_2O)_2$ complexes are respectively: -1.2393, -1.2314, -1.1610 and -1.1723 Hartrees. The examination of these negatives values indicates that the metal-ligands complexation was thermodynamically favored in all investigated complexes and the $Mn(L^1)_2(H_2O)_2$ complex has the highest binding energy (encompassing coordination and electrostatic bonds).

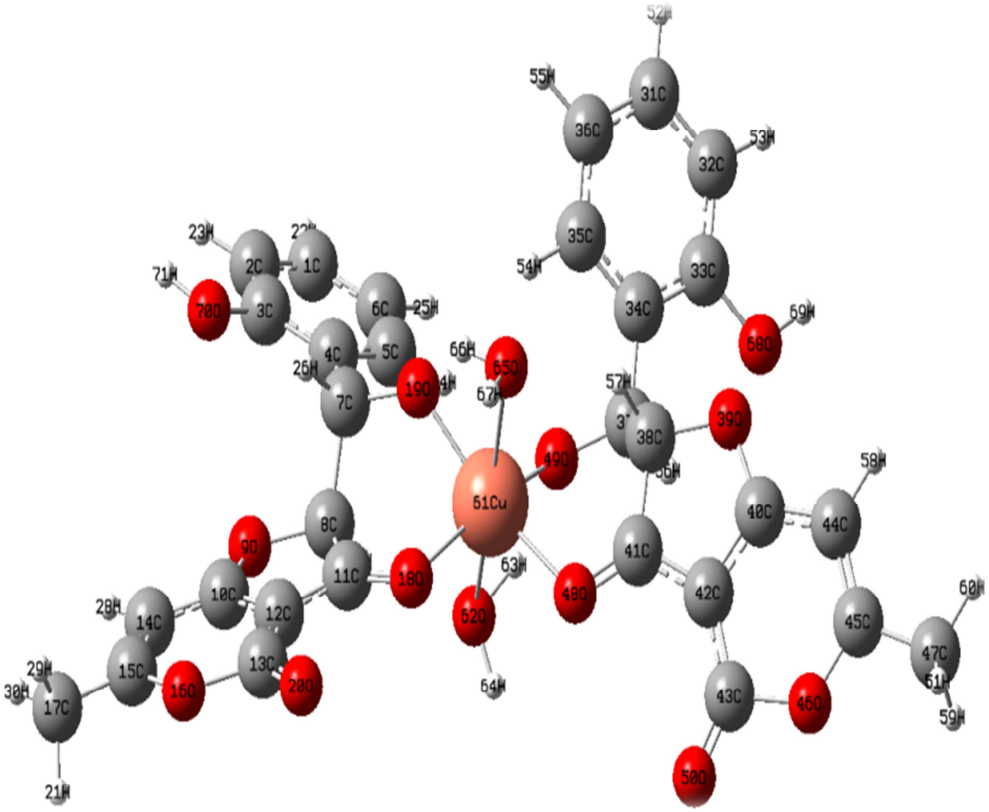

Fig.6. Structure of $[Cu(L^2)_2(H_2O)_2].H_2O$ optimized at DFT method.

5.3 Electronic spectra:

The UV-vis spectra of manganese complexes do not reveal bands due to d-d transitions within the metal because the orbital d of metals are saturated and d-d transitions are not permitted [48-49]. The absence of d-d transition band for these complexes suggest the (+II) oxidation state for manganese ion [50-52].

The spectra of these manganese complexes in DMSO solution (10^{-3}M) give a band at 21186 cm^{-1} (472 nm), 22624 cm^{-1} (442 nm) for the complexes [Mn $(L^1)_2$ $(H_2O)_2$].H_2O and [Mn$(L^2)_2(H_2O)_2$].H_2O respectively, which might be assigned to charge transfer transition L→M (CT). Intense absorption bands were observed on the spectra of complexes in the ultraviolet range (see figures 7 and 8). They are due to intra-ligand transitions $\pi \rightarrow \pi^*$ and $n \rightarrow \pi^*$. The appearance of intra-ligand bands shows the existence of the ligand within the complex. The suggested band (cm^{-1}) assignments of manganese (II) and copper (II) complexes and molar absorption coefficients are summarized in Table 2. The electronic absorption spectra of the copper complexes recorded in DMSO solution (10^{-3}M) reveal three bands in the visible range, the first appears in the field 14045-15361 cm^{-1} interval, assigned to the $^2B_{1g} \longrightarrow {}^2B_2g$ transition, the second strongest intensity located around 14740-17857 cm^{-1} region attributed to the $^2B_{1g} \longrightarrow {}^2Eg$ transition [53-55]. A third band observed in the 22427– 27027 cm^{-1} region for these complexes refers to L→M (CT) band. These transitions are characteristic of octahedral symmetry around the Cu (II). The characteristics of these bands are summarized in Table 2.

Table 2: The main absorbance bands (cm^{-1}) in UV–vis spectra and their assignments of manganese (II) and copper complexes.

Complexes	*Wave Number* $\bar{\nu}$ *(cm^{-1})*	*Wave length* λ *(nm)*	*Molar coefficient absorption* *(ε : l. $mole^{-1}.cm^{-1}$)*	*Electronic transitions*
$[Cu(L^1)_2(H_2O)_2].H_2O$	44248	226	22500	$\pi \longrightarrow \pi^*$
	32895	304	12000	$n \longrightarrow \pi^*$
	22472	445	320	Charge transfer
	14045	712	102	$^2B_{1g} \longrightarrow {}^2B_2g$
	14749	678	112	$^2B_{1g} \longrightarrow {}^2Eg$
$[Cu(L^2)_2(H_2O)_2].H_2O$	44643	224	12800	$\pi \longrightarrow \pi^*$
	32787	305	5460	$n \longrightarrow \pi^*$
	27027	370	460	Charge transfer
	15361	651	23	$^2B_{1g} \longrightarrow {}^2B_2g$
	17857	560	34	$^2B_{1g} \longrightarrow {}^2Eg$
$[Mn(L^1)_2(H_2O)_2].H_2O$	44248	226	22500	$\pi \longrightarrow \pi^*$
	32895	304	12000	$n \longrightarrow \pi^*$
	21186	472	423	Charge transfer
$[Mn(L^2)_2(H_2O)_2].H_2O$	44643	224	12800	$\pi \longrightarrow \pi^*$
	32787	305	5460	$n \longrightarrow \pi^*$
	22624	442	312	Charge transfer

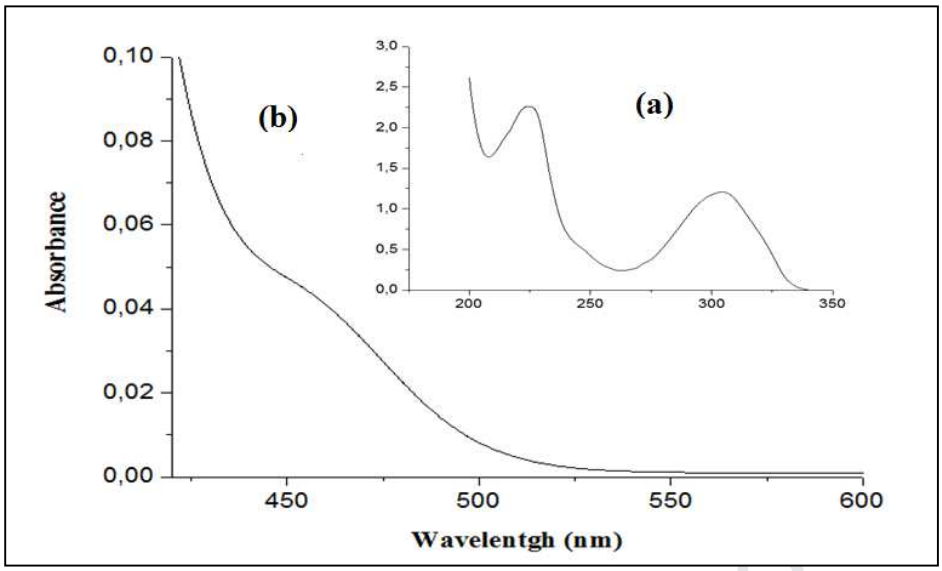

Fig.7. Electronic spectra of **(a)** L^1 and **(b)** $[Mn(L^1)_2(H_2O)_2].H_2O$ complex.

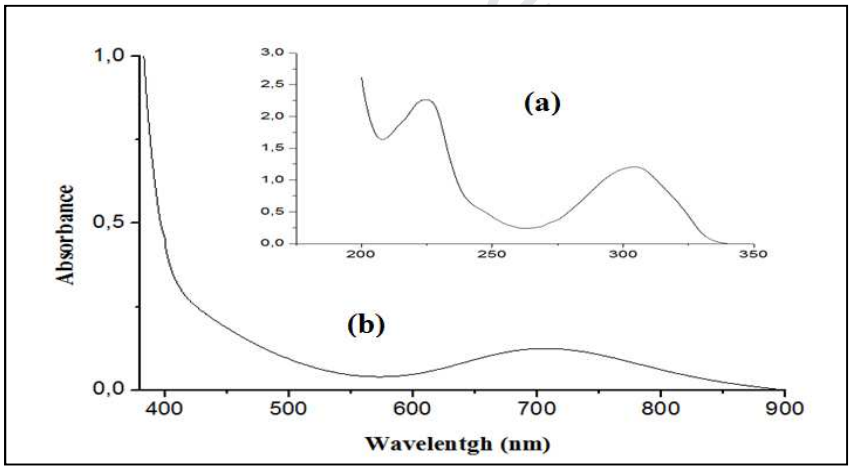

Fig.8. Electronic spectra of **(a)** L^1 and **(b)** $[Cu(L^1)_2(H_2O)_2].H_2O$ complex.

5.4 IR spectra and mode of bonding:

The determination of the coordinated atoms was made on the basis of the comparison of the IR spectra of the ligands and those of complexes. Significant wave numbers are grouped in Table 3. The engagement of these ligands in the bonds with the metal center affects the vibrations of the bonds of the donor atoms (oxygen) with the neighboring atoms. In the large wavenumber domain 3400-3300 cm^{-1}, a wide band appears attributed to the vibrations of the O-H bonds of hydration water molecules. The vibration of the bond ($C = O_1$) of the furanone ring has shifted after complexation towards the large wavenumbers. This result indicates that the oxygen of the furanone ring is involved in the

complexation. The IR spectra of the complexes are characterized by the disappearance of the vibration band of the O-H bond indicating the deprotonation of the ligand after complexation and the formation of the neutral complexes. Then, the oxygen atoms of the two ligands are engaged in the bond with the central metal, this is confirmed by the appearance of new bands of vibrations towards the low energies in the 455 and 411 cm^{-1} domain due to the formation of metal-ligand bonds [58-59]. The theoretical IR spectra obtained at the DFT method for the copper and manganese complexes show a close resemblance to the corresponding experimental spectral bands. On the basis of the results obtained by spectroscopic investigations we suggest that the ligands are coordinated in both sites: deprotonated oxygen and carbonyl moiety leading to neutral complexes. The ligands coordination sites which are involved in bonding with the metal ions have been determined by careful comparison of the infrared absorption spectra of the complexes with those of the parent ligands. The main absorbance bands in experimental and calculated IR spectra and their vibrational assignments for four complexes are presented in Table 3. The experimental and theoretical IR spectra of selected $[Mn(L^1)_2(H_2O)_2].H_2O$ and $[Cu(L^2)_2(H_2O)_2].H_2O$ complexes are illustrated in Fig.9 and Fig.10. These spectra were used to confirm the experimental assignments.

Table 3: The main absorbance bands (cm^{-1}) in experimental and calculated FT-IR spectra and their assignments for four complexes.

Compound	$\bar{\nu}_{(OH)}$ [a]	$\bar{\nu}_{(OH)}$ [b]	$\bar{\nu}$ C=O str. Pyrone-2	$\bar{\nu}$ C=O	$\bar{\nu}$ (M-O1)	$\bar{\nu}$ (M-O2)
L^1						
$[Mn(L^1)_2(H_2O)_2].H_2O$	3600	3434 (3641)	1752 (1743)	1780 (1743)	413 (439)	450 (457)
$[Cu(L^1)_2(H_2O)_2].H_2O$	3565	3360 (3226)	1760 (1790)	1783 (1621)	411 (437)	443 (464)
L^2						
$[Mn(L^2)_2(H_2O)_2].H_2O$	3554	3411(3267)	1742(1792)	1781 (1798)	422(438)	455 (468)
$[Cu(L^2)_2(H_2O)_2].H_2O$	3595	3370 (3173)	1751 (1637)	1785 (1787)	416 (412)	449 (463)

a: H_2O Hyd, b: H_2O coord, (M-O1): oxygen of furanon ring, (M-O2): oxygen of deprotonated OH.
The calculated values of main absorbance bands are indicated in parenthesis.

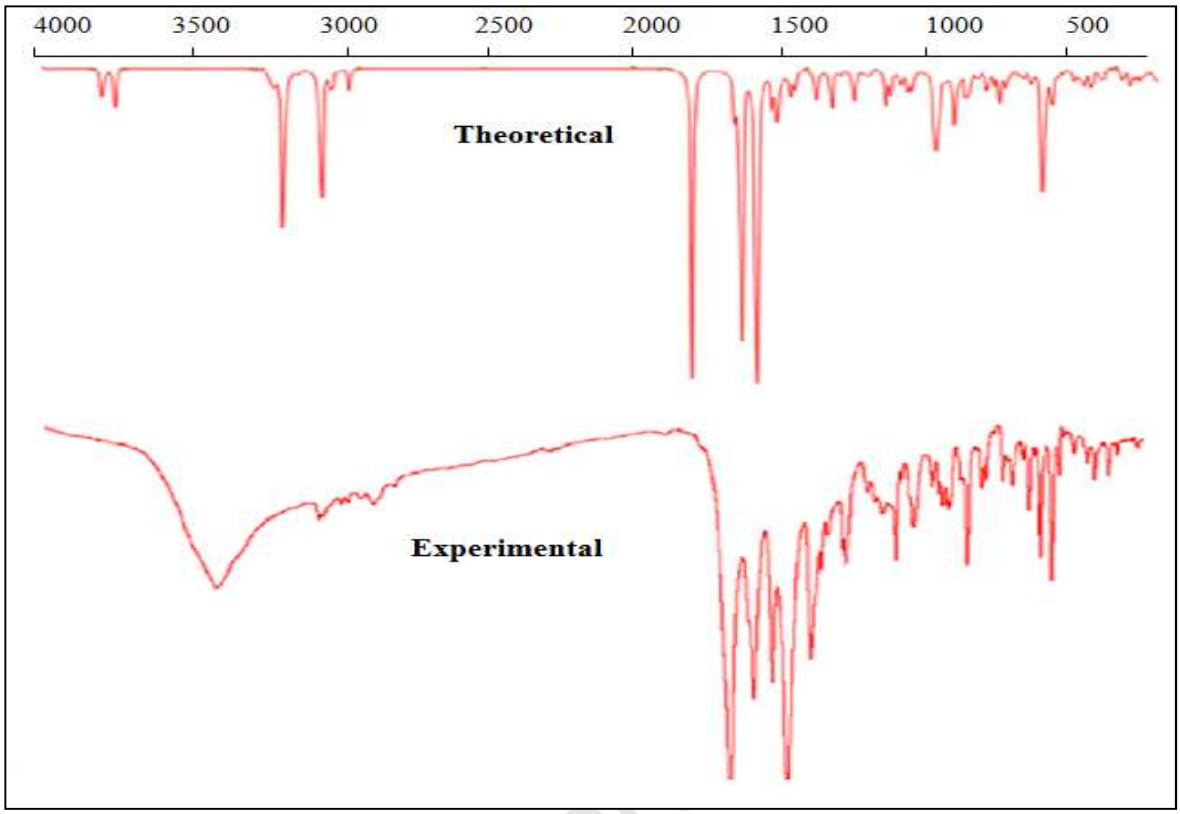

Fig.9. Experimental and theoretical IR spectrums of [Mn $(L^1)_2(H_2O)_2$].H_2O complex

The experimental vibrational frequencies of hydroxyl water group (H_2O of coordination) were found in the range 3434-3411 cm^{-1} 3360-3370 cm^{-1} for manganese and copper complexes respectively for both L^1 and L^2 ligands. The calculated values are as follow: 3641 and 3267 cm^{-1} for manganese complex and 3226 and 3173 cm^{-1} for copper complexes (see table 3). A broad band of m(OH) group in the experimental IR spectra is observed at 3390 and 3480 cm^{-1} for both L^1 and L^2 free ligands. These band are absent in the spectra of manganese and copper complexes, suggesting the deprotonation of the L^1 and L^2 ligands. The lack of this band in spectra of complexes proves a result of complex formation. This result was also discussed in the experimental IR investigation. The bands with medium intensity observed in the range 3200-3650 cm^{-1} of the manganese complexes are attributed to m(OH) of coordinated water. The experimental value of C=O (pyrone-2) absorption band is in the range 1748-1756 cm^{-1} for both free ligands.

This vibration is shifted to the lower regions in the Mn complexes indicating the formation of a bond between the metal ion and the C=O group, while the theoretical values are established in the range 1743-1792 cm^{-1} as calculated by B3LYP method. In copper complexes, the C=O band absorption appears at 1760 and 1751 cm^{-1} respectively for [Cu$(L^1)_2(H_2O)_2$].H_2O and [Cu$(L^2)_2(H_2O)_2$].H_2O and their corresponding calculated values

are 1790 cm^{-1} and 1637 cm^{-1}. Then, reasonable agreement between the theoretical and experimental results for M-O_1 and M-O_2 vibrations bands (as indicated in the same table) reflects well the suitability of DFT method for this type of study. Hence, this careful spectral investigation indicates that both ligands act as a bidentate anion and that the coordination is through the oxygen donor atoms of the carbonyl group and the charged oxygen resulting of deprotonated hydroxyl moiety. In general, the absorption frequencies obtained from IR experiment spectrum of the four synthesized organometallic complexes and theoretical calculations are in good agreement.

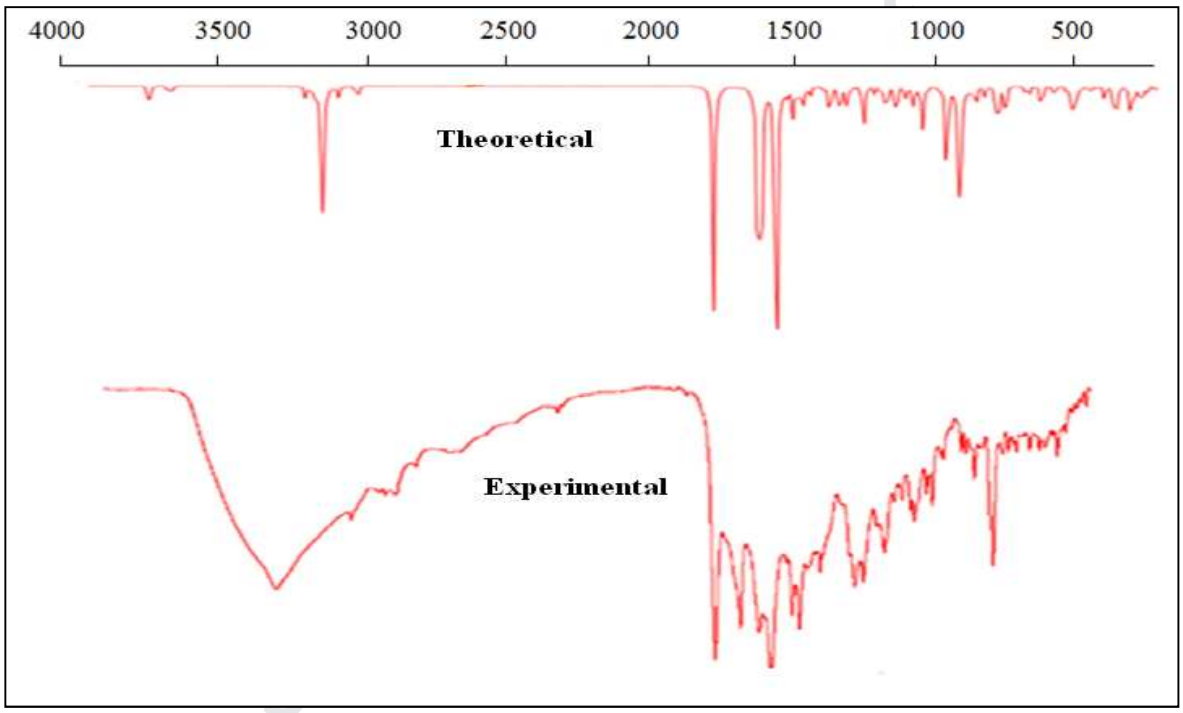

Fig.10. Experimental and theoretical IR spectrums of [Cu $(L^2)_2(H_2O)_2$].H_2O complex

5.5 Electronic spin resonance (ESR):

5.5.1 *Manganese complexes:*

The ESR spectra of manganese (II) complexes in solid state at room temperature show a strong signal centered at g = 2 (Fig. 11), which is associated with I = 5/2 nuclear spin of ^{55}Mn. The resonance at this value is due to Mn(II) ions in an environment close to octahedral symmetry. These spectra confirm that they are high-spin Mn (II) complexes [50].

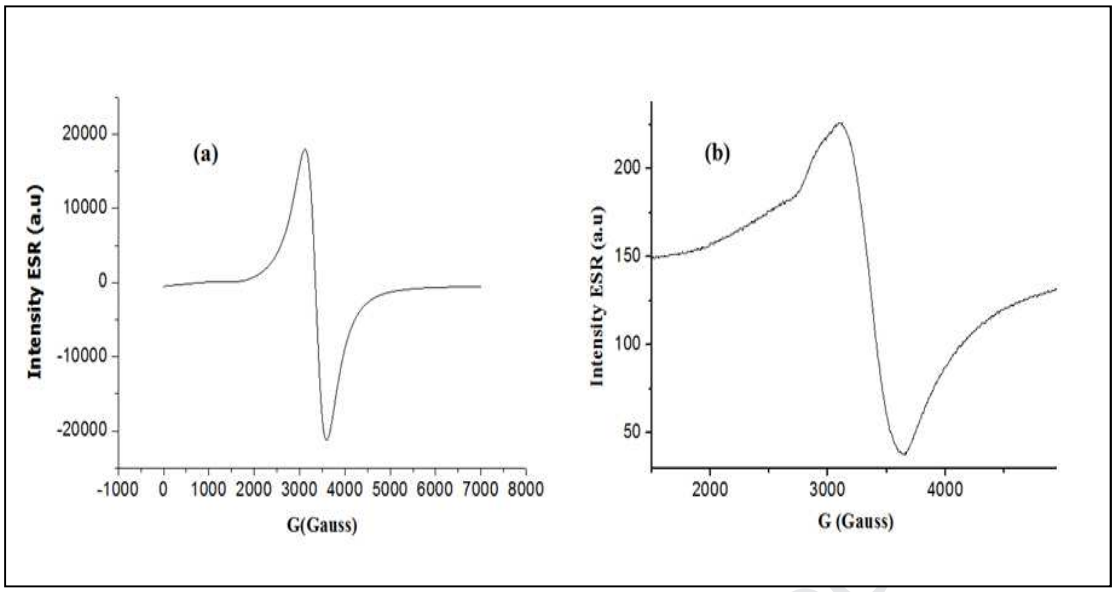

Fig. 11. ESR powder spectra of **(a)** $[Mn(L^1)_2(H_2O)_2].H_2O$ and **(b)** $[Mn(L^2)_2(H_2O)_2]. H_2O$

5.5.2 Copper complexes:

The ESR spectra of the copper (II) complexes were recorded in solution in the DMSO at T = 115 K. The parameters g//, $g_\perp$ and A// determined from the experimental spectra are grouped in Table 4. As the $\perp$ lines are not resolved $A_\perp$ has not been calculated. The hyperfine structure is well resolved for the four complexes (Fig.12). It consists of four hyperfine lines attributed to the interaction of the single electron with the Cu nucleus (I = 3/2). The values obtained for all the parameters show that the spectra of the two complexes have an axial symmetry with: g// > $g_\perp$ > 2,0023, this order is typical of monomeric Cu (II) complexes and indicates that the single electron is located on the orbital d_{x2-y2} of the Cu (II) ion and confirmed an octahedral geometry [60-62]. To better define the nature of the links formed, several Bonding parameters α^2 (covalent in-plane δ-bonding), β^2 (covalent in plane π-bonding) and γ^2 (covalent out of plane π -bonding) were evaluated using the following formulas:

$$\alpha^2 = (A_{//}/0.036) + (g_{//} - 2.0023) + 3/7(g_\perp - 2.0023) + 0.04]$$

$$\alpha^2\beta^2 = \frac{[(g_{//} - 2.0023)\Delta_{//}]}{8\lambda_0} = K^2_{//}$$

$$\alpha^2\gamma^2 = \frac{[(g_\perp - 2.0023)\Delta_\perp]}{2\lambda_0} = K^2_\perp$$

Where λ_0 is the constant of spin orbit coupling, for copper (II): λ_0 = - 828 cm^{-1}, $\Delta_{//}$ and $\Delta_{\perp}$ are the energies of the transitions $^2B_{1g} \longrightarrow {}^2B_2g$ and $^2B_{1g} \longrightarrow {}^2Eg$, respectively.

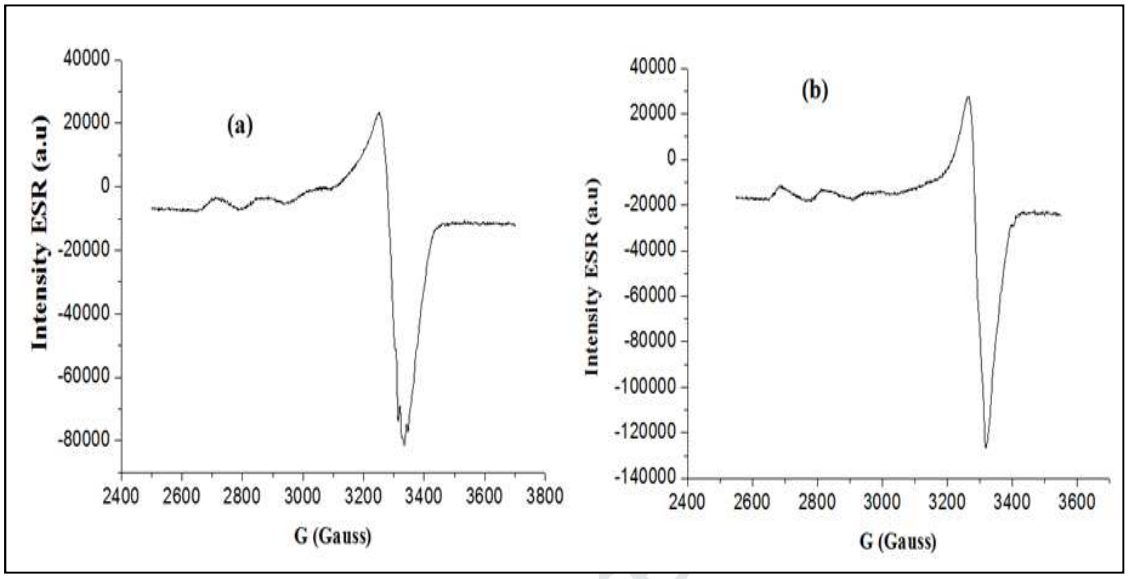

Fig.12. ESR spectra of **: (a)** $[Cu(L^1)_2(H_2O)_2].H_2O$ and **(b)** $[Cu(L^2)_2(H_2O)_2].H_2O$) in DMSO solution at 115 K.

α^2 and β^2 respectively represent the metal-ligand bonding parameters σ and π in the plane and γ^2 represents the bond π out of plane. The product values $\alpha^2\beta^2$ and $\alpha^2\gamma^2$ measure the covalence of the combined σ and π bonds. They range from 1.0 to 0.25; the first value corresponds to a 100% ionic character and the second to a 100% covalent character respectively [50, 63]. The values obtained for our complexes (see Table 4) show a greater covalent character for the metal-ligand bonds outside the plane. It has been noted that the $\alpha^2\beta^2$ covalent character increases in the Cu-L^2 < Cu-L^1 order for the L^1 and L^2 ligands. This order correlates with the increase in the donor effect of the R substituent.

Table 4: ESR data of the copper complexes.

Complexes	$g_{//}$	$g_{\perp}$	$A_{//}$ $\times 10^{-4}$ cm^{-1}	$\alpha^2\beta^2$	$\alpha^2\gamma^2$	$K_{//}$	$K_{\perp}$
$[Cu(L^1)_2(H_2O)_2].H_2O$	2.31	2.06	145	0.652	0.514	0.807	0.717
$[Cu(L^2)_2(H_2O)_2].H_2O$	2.33	2.06	150	0.760	0.622	0.871	0.788

5.6. Frontier orbital molecular and charge transfer:

For further investigations, energies of HOMO and LUMO are popular quantum mechanical descriptors. It has been shown [64] that these orbitals play a major role in governing various chemical reactions, and are also responsible for charge transfer complexes. The treatment of the frontier molecular orbitals, separately from the other orbitals, is based on the general principles governing the nature of chemical reactions. The concept of hard and soft nucleophiles and electrophiles has been also directly related to the relative energies of the HOMO and LUMO orbitals. Soft nucleophiles have an elevated energy HOMO, hard nucleophiles have a small energy HOMO, soft electrophiles have a low energy LUMO and hard electrophiles have a high energy LUMO [65]. Thus, HOMO–LUMO energy gap is an essential stability indicator [66]. The energies of the LUMO and HOMO for different partners are evaluated in Free State and for four complexes using DFT method.

The distribution of charge density of the two frontier molecular orbitals for the free molecule ligands L^1 and L^2 are presented in Fig.13 and 14. As we can see, in the Free State the high density of the HOMO distribution is concentrated on pyranone ring group. The low and high electronic densities are distributed on the same group in the case of LUMO orbital [67]. The calculated values of HOMO and LUMO energies of the four complexes are also presented in the same Fig.13 and 14. The LUMO of $[Cu(L^1)_2(H_2O)_2]$ complex is located on the both pyranone groupement thus the HOMO is located on phenylics moieties. In $[Cu(L^2)_2(H_2O)_2]$ the same shape of HOMO and LUMO are obtained.

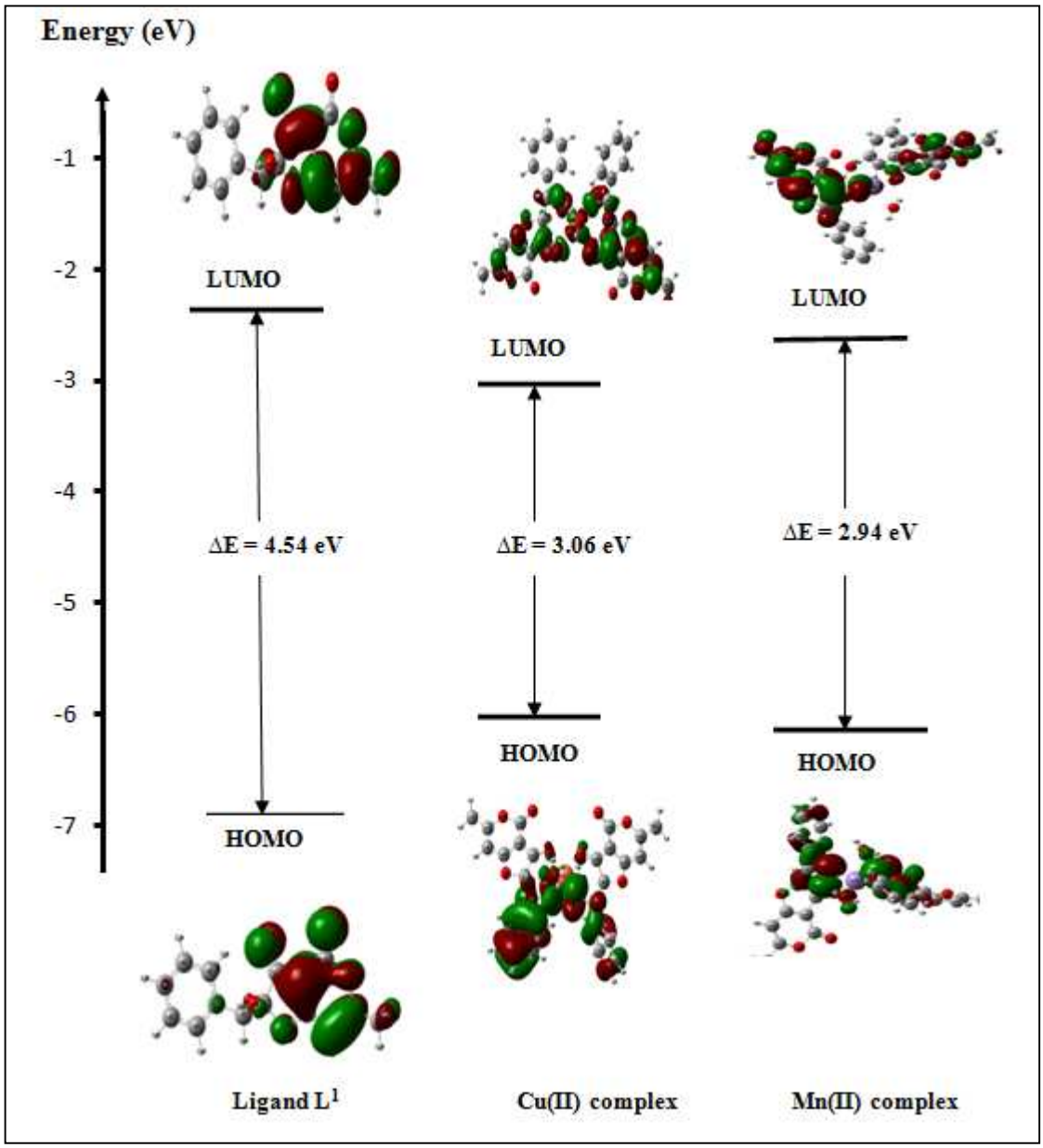

Fig.13. The HOMO, LUMO energy structures of isolated and complexed Ligand L^1 in both complexes obtained by the DFT calculations**.**

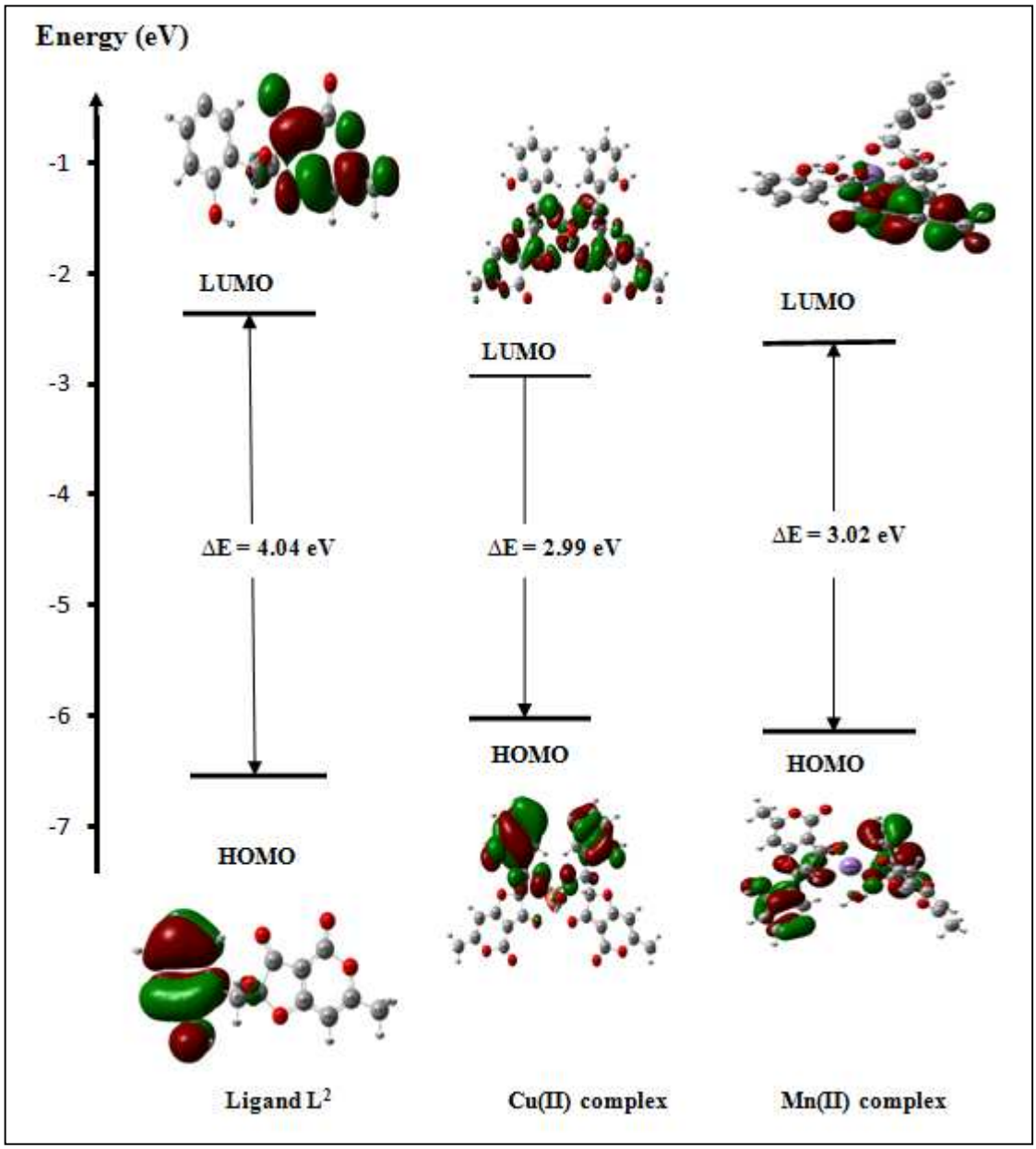

Fig. 14. The HOMO, LUMO energy structures of isolated and complexed Ligand L^2 in both complexes obtained by the DFT calculations.

The values of the HOMO–LUMO energy gap , estimated for the copper and manganese complexes are equal to 3.06 eV, 2.99 eV , 2.94 eV and 3.02 eV respectively for $[Cu(L^1)_2 (H_2O)_2]$, $[Cu(L^2)_2 (H_2O)_2]$, $[Mn(L^1)_2 (H_2O)_2]$ and $[Mn(L^2)_2 (H_2O)_2]$. HOMO–LUMO turned out is 4.54 ev and 4.04 eV respectively for the L^1 and L^2 ligands which is greater than those of the four complexes. The decrease in the HOMO-LUMO energy gap after complexation explains the potential for charge transfer interactions taking place between both donor-acceptor partners, which may be responsible for the bioactivity of the

consequential molecules [67, 68]. The target ligands exhibit an effective intermolecular charge transfer with metallic ions. Therefore, we can say that the complexation doesn't affect dramatically the electronic properties of both ligands. In consequence, the greater the energy gap is, the higher the stability is.

5.7 Analysis of molecular electrostatic potential:

The electrostatic potential that is created in the space around a molecule by its electrons and nuclei is a very useful property for analyzing and predicting molecular reactive behavior [69, 70]. The molecular electrostatic potential surface (MEP) gathers a lot of information as follow: molecules dipole moments, molecular shape, and the distribution of electrostatic potential. It provides an illustration method to understand the relative polarity of a molecule. The sites for electrophilic and nucleophilic attacks of the molecules can be determined with the help of the molecular electrostatic potential. The different values of the electrostatic potential at the surface are represented by different colors. The MEP color scheme reflects the electron-rich and electron-poor areas, the meaning is: the blue color corresponds to the electron deficient or partially positive charge, the red color corresponds to the rich sites in electrons and both intermediate colors: yellow and light blue are respectively corresponding to the slightly electron loaded region and slightly electron poor region.

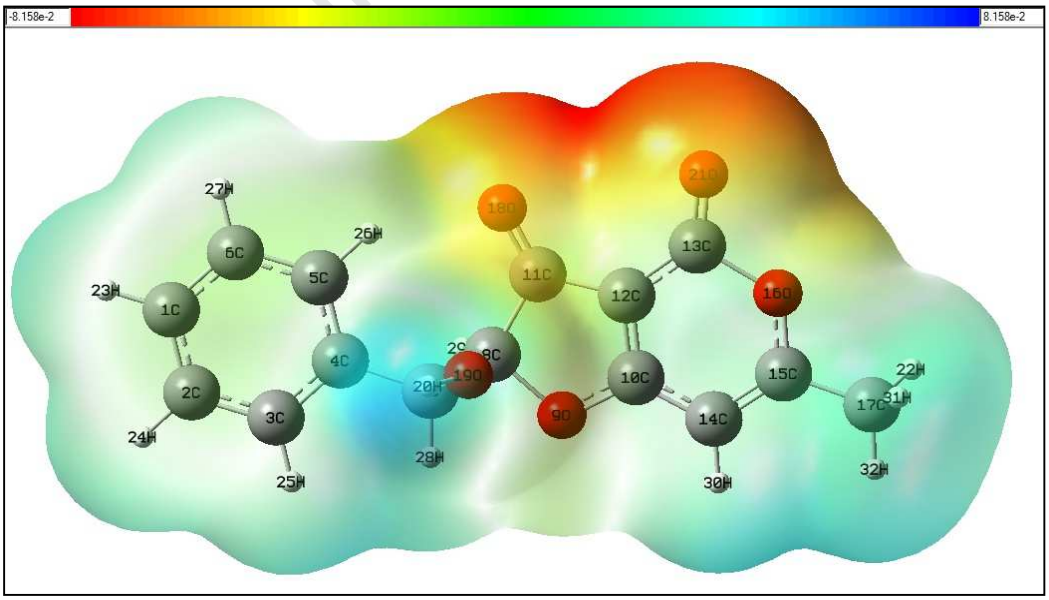

Fig.15. The total electron density surface of free L^1 ligand

The SCF (Self Consistent Field) of surface electron density traced with MEP of the compound is shown in Figure 15. The total electron density varies between two extreme limits: $-8.158.10^{-2}$a.u to $+8.158.10^{-2}$ a.u. As can be seen from the Molecular electrostatic potential map of the free ligand, the negative regions are mainly localized on the oxygen atoms, O16, O21 and O18 atoms where the corresponding electron densities are respectively: $-5.007.10^{-2}$ a.u, $-7.06.10^{-2}$ a.u, and $-7.15.10^{-2}$a.u and slight electron rich region for Ol9 is -2,50 $.10^{-2}$ a.u. As well the most electron deficient region is around phenilic group and the slightly electron efficient region is around methylic group where the electron density is $+3.36.10^{-2}$ a.u. Then, the electron density reveals the polarity of the molecule. The MEP clearly indicates the electron poor region of the ligand. In parallel, fig.16 shows the total electronic density of $[Cu(L^1)_2(H_2O)_2]$ complex (selected). The limit values are between $-6.817.10^{-2}$ a.u and $+6.817.10^{-2}$ a.u. As can be seen, the electron rich regions are located in carbonyl groups and electron poor regions in phenilic and methylic groups.

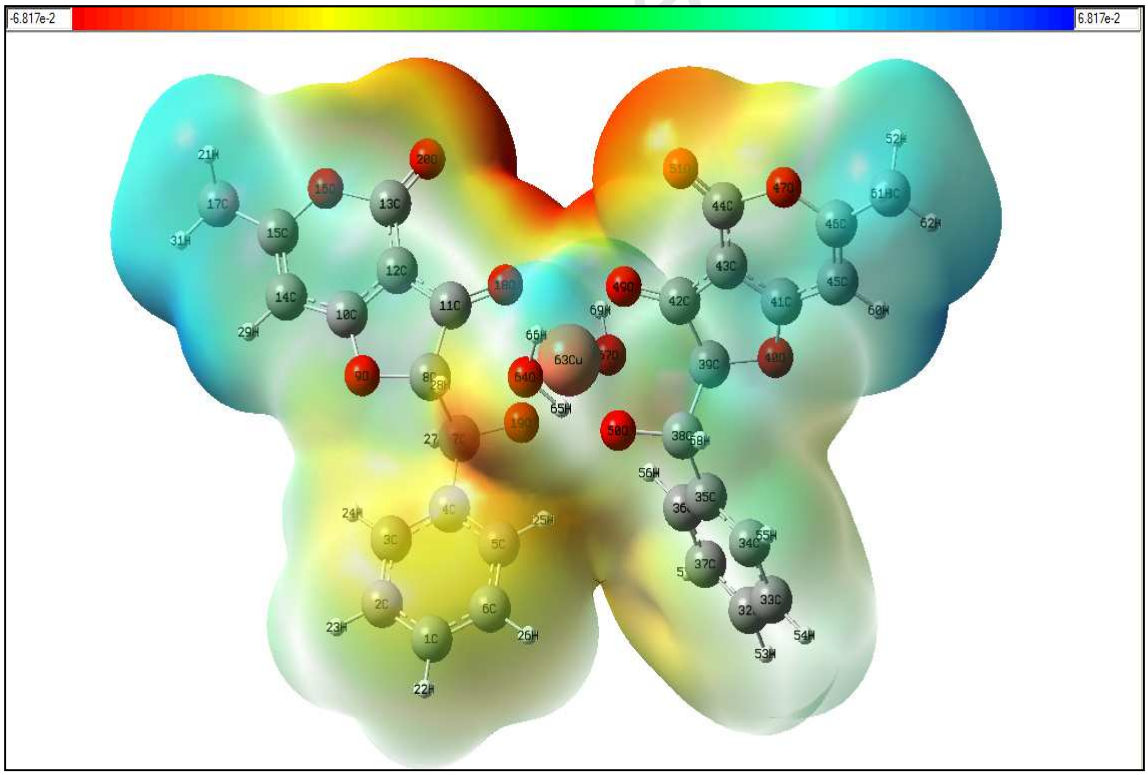

Fig.16. The total electron density surface of $[Cu(L^1)_2(H_2O)_2]$ complex.

5.8 Electronic spectra : TD-DFT calculations

Electronic structures are fundamental for the interpretation and understanding of the absorption spectra [46]. The UV-vis absorption spectra were calculated on optimized geometries. Then, TD-DFT calculation on the four complexes in DMSO as selected solvent have been carried out using UB3LYP/LanL2DZ level of DFT method. The Comparison of the theoretical λ_{max} of complexes with the experimental wavelength λ_{max} values is presented in Table 5. The oscillator strength (f) which is a dimensionless quantity was used to express the transition probability of the Charge Transfer band. The oscillators's strengths of the observed transitions in copper (II) complexes are small. This obtained result is a characteristic of spin allowed and symmetry forbidden d–d transitions [57]. We can also notice that there is a reasonable agreement between the experimental and calculated values of λ_{max}. The experimental and calculated results of UV–vis spectral data were compared in Table 3.

Table 5: Wavelengths λ_{max}, oscillators strengths (*f*) and main electronic transitions of the studied complexes.

Complexes	***λ_{exp} (nm)***	***λ_{cal} (nm)***	***f***	***main electronic transition***
$[Mn(L^1)_2(H_2O)_2]$	**472**	**507**	**0.0432**	Charge transfer
$[Mn(L^2)_2(H_2O)_2]$	**442**	**478**	**0.0269**	Charge transfer
$[Cu(L^1)2(H_2O)_2]$	**712**	**675**	**0.0017**	d-d electronic transition
	678	**602**	**0.0004**	d-d electronic transition
$[Cu(L^2)_2(H_2O)_2]$	**651**	**691**	**0.0006**	d-d electronic transition
	560	**597**	**0.0008**	d-d electronic transition

The theoretical results have shown that TD-DFT calculations, with a hybrid B3LYP functional in conjunction with CPCM of solvation together with a LanL2DZ basis set, was clearly able to predict the excitation energy and the absorption spectrum of the studied molecules. From figures 17 and 18 (for the selected Mn complexes), and taking into account the maximum absorbance positions, the simulated spectrums of the two selected complexes showed a good agreement with the experimental results.

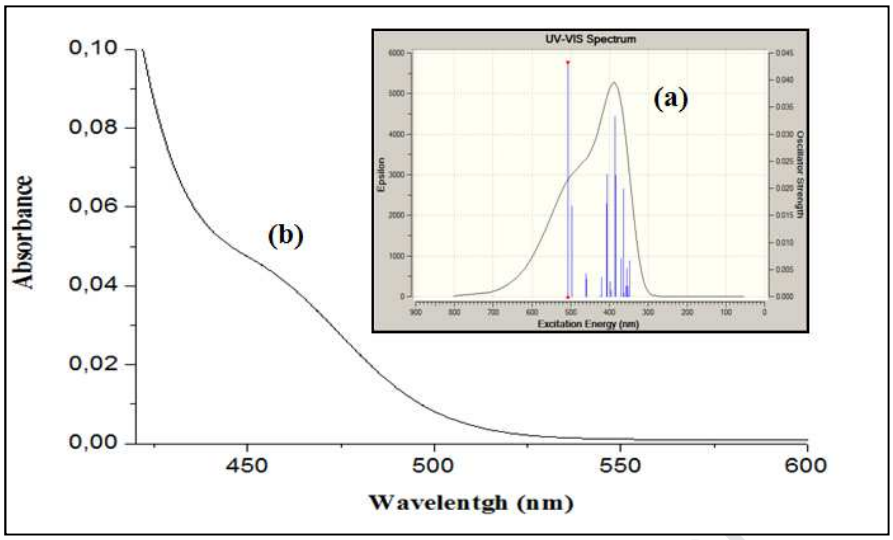

Fig.17. UV-vis spectra of $[Mn(L^1)_2(H_2O)_2]$; **(b)** experimental; **(a)** TD-DFT spectrum.

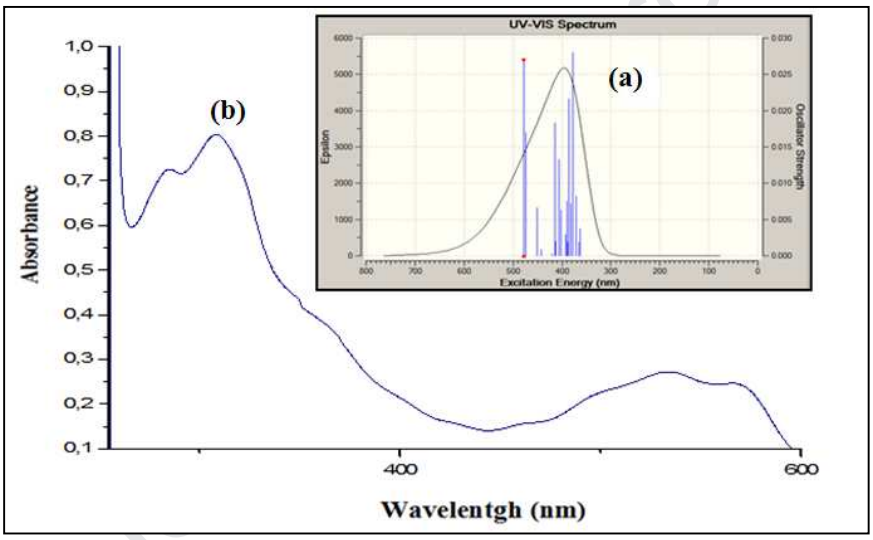

Fig.18. UV-vis spectra of $[Mn(L^2)_2(H_2O)_2]$; **(b)** experimental; **(a)** TD-DFT spectrum.

6. Antibacterial and antifungal activities (in vitro):

The antimicrobial activity of ligands and their metal complexes has been studied in vitro against fungi and pathogenic bacteria in DMSO. We performed these tests by the disk diffusion method; the results are given in Figs. 19 and 20. It is of note that for the activity of both standard references with the selected bacteria, the diameters of the inhibition zones (measured in millimeter at 24 hours) of *Echerichia coli and Klebsiella pneumoniae* bacteria with cefotaxime are respectively: 35 mm and 20 mm, and that of *Staphylococcus aureus* and *group D Streptococcus* with gentamicine is 40 mm. Compared with the standards data, the tests reveal that the newly prepared ligands and their metal complexes

showed an interesting effect against most microorganisms. However, the antimicrobial screening data show that L^1 and L^2 ligands are more active against Gram-positive bacteria than Gram-negative bacteria.

The high resistance of gram (-) bacteria is related to the complexity of the cell wall of these microorganisms which contains a double membrane, unlike the simple membrane structure of gram (+) bacteria [71]. The manganese complex (MnL^1) has shown excellent antibacterial activity against gram-positive bacteria (*Staphylococcus aureus, group D Streptococcus)* and gram-negative bacteria (*Klebsiella pneumaniae*) and moderate activity against Gram-negative bacteria (*Echerichia coli).*

The copper complex with the ligand L^1 (CuL^1) showed an important activity than that of the ligand L^1 namely an excellent antibacterial activity against gram-positive bacteria (*Staphylococcus aureus*, *group D Streptococcus*) and a moderate activity against bacteria (*Echerichia coli*, *Klebsiella pneumaniae)* to Gram negative. The interesting activity of copper and manganese complexes can be explained by the theory of chelation [50, 72]. The Chelation reduces the polarity of the central metal atom due to the partial sharing of its positive charge with the ligand, which promotes the penetration of the complexes by the lipid layer of the cell membrane [73-76].

The copper and manganese complexes with the L^2 ligand exhibit activity relative to that of ligand L^2 with respect to the bacteria tested. It should be noted that the MnL^2 and CuL^2 complexes have a good antibacterial activity particular to the bacterium *group D Streptococcus*. In general, the copper and manganese complexes derived from the L^1 ligand are more active than the L^2 ligand complexes. In addition, the activity studies indicated that MnL^1 complex exhibited activity better than standard antibiotic Cefotaxime against *Klebsiella pneumaniae*. This is well justified by its diameter of the inhibition zones which reached 36 mm. These results indicate that the type of substitution in the benzoic ring has a significant influence on antibacterial activities. This antimicrobial behavior is related to the electronic effect of the substituents [77].

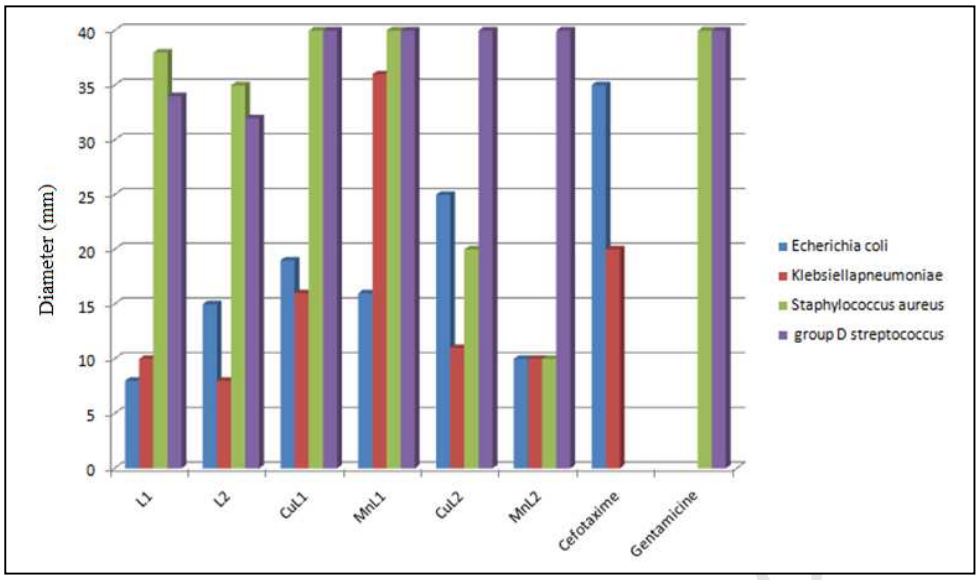

Fig. 19. Comparison of antibacterial activity of compounds.

The disk diffusion method also allowed us to determine the antifungal power of the two ligands and the four complexes with respect to *Candida albicans and Candida tropicalis*. In these tests, the diameters of the inhibition zones of ketokonazole used as standard reference for *Candida albicans* and for *Candida tropicalis* are respectively 33mm and 35 mm (see figure 20). Based on standard values, we find that the ligands and their metallic complexes exhibit excellent antifungal activity against *candidas* previously mentioned and were more potent than ketokonazole. In parallel, the synthesized coordination complexes showed a clear improvement of the antifungal tests in comparison with those of the free ligands.

Therefore, it is clear from Figure 20 that the four complexes are very active against both selected candidas (a value of 40 mm for the four complexes). This indicates that the chelation in the case of manganese and copper complexes increases the lipophilic nature of the nucleus. However, the results relating to the measurement of inhibition diameters of mycelial growth show that the tested ligands and their complexes have a high antifungal power.

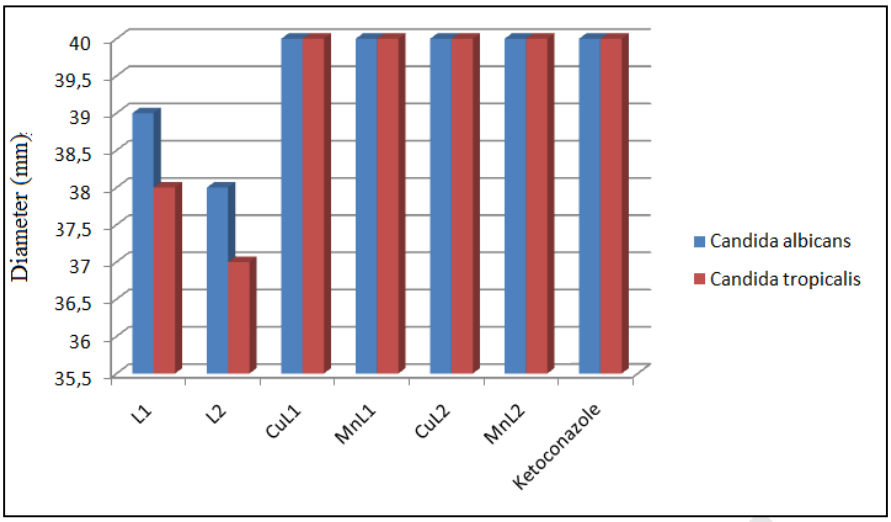

Fig. 20. Comparison of antifungal activity of compounds.

In conclusion, the obtained biological tests indicated that the new synthesized ligands and their four complexes exhibited a broad spectrum of activity against the tested bacteria and fungi strains and these encouraging results allow us to pave the way for more advanced biological tests (anti inflammatory, oncostatic…..).

7. Conclusion:

The synthesis and characterization of new copper (II) and manganese (II) complexes with two new furopyran-3, 4-dione ligands are reported. The UV–Vis electronic absorption and IR spectral data of the four synthesized complexes have been compared with the results obtained by theoretical calculations, the results of these calculations showed a good agreement with the experimental results. The ESR spectral data of the copper complexes indicate that the complexes have axial symmetry, which also confirms the oxidation states of the metal ions. The different characterizations allowed assigning coordination six for the obtained complexes. Elemental analysis revealed the geometry of these complexes whose general formula is $[M(L)_2(H_2O)_2].nH_2O$. The calculated geometric parameters confirmed the distorted octahedral geometry of the studied complexes. Antibacterial and antifungal activities of ligands and their Cu (II) and Mn (II) complexes were evaluated in vitro against different antibacterial and antifungal strains. The antifungal activity of ligands and their metal complexes gave interesting result. The chelates and the ligands are found to have an excellent antifungal activity against *Candida albicans* and *Candida tropicalis*. This finding indicated to very promising candidates as antimicrobial new products because they will almost certainly be important in the development of beneficial new drugs.

Acknowledgments:

This study was supported by the Algerian minister of higher education and scientific research through the CNEPRU research grants.

References:

[1] J. Costmagna, J. Vargas, R. Latorre, A. Alvardo and G. Mena, Coordination compounds of copper, nickel and iron with Schiff bases derived from hydroxynaphthaldehydes and salicylaldehydes, Coord, Chem. Rev. 119 (1992) 67-88.

[2] Y. S. SHARMA, H. N. Pandey and P. Mathur, Monomeric and dimeric copper(II) coplexes of a redox active Schiff base ligand bis(2,5-dihydroxyacetophone) ethylenediamine.Polyhedron, 13 (1994) 3111-3117.

[3] D.P. Kessissoglou, Homo- and mixed-valence EPR-active trinuclear manganese complexes. Coord. Chem. Rev. 186 (1999) 837–858.

[4] M-X. Li, C. Chen, D. Zhang, J. Niu, B-S. Ji, Mn(II), Co(II) and Zn(II) complexes with heterocyclic substituted thiosemicarbazones: synthesis, characterization, X-ray crystal structures and antitumor comparison, Eur. J. Med. Chem. 45 (2010) 3169–3177.

[5] S. Mandal, A. Rout, A. Ghosh, G. Pilet, D. Bandyopadhyay, Synthesis, structure and antibacterial activity of manganese (III) complexes of a Schiff base derived from furfurylamine, Polyhedron 28 (2009) 3858–3862.

[6] D. P. Singh, K. Kumar, C. Sharma, New 14-membered octaazamacrocyclic complexes: Synthesis, spectral, antibacterial and antifungal studies, Eur. J. Med. Chem. 45 (2010) 1230–1236.

[7] M. Chen, S. Lin, L. Li, C. Zhu, X. Wang, Y. Wang, Enantiomers of an indole alkaloid containing unusual dihydrothiopyran and 1,2,4-thiadiazole rings from the root of *Isatis indigotica*. Org Lett. 14 (2012) 5668–5671.

[8] T. Akizawa, T. Yasuhara, H. Azuma, T. Nakajima, Novel polyhydroxylated cardiac steroids in the nuchal glands of the snake, Rhabdophis tigrinus, Biomed. Res. 6 (1985) 437-441.

[9] S. Azuma, S. Sekizaki, T. Akizawa, T. Yasuhara, T. Nakajima, Activities of novel polyhydroxylated cardiotonic steroids purified from nuchal glands of the snake, Rhabdophis tigrinus, J. Pharm. Pharmacol. 38 (1986) 388-390.

[10] H. G. Cutler, J. M. Jacyno, Biological Activity of (-)-Harzianopyridone Isolated from Tvichoderma harzianum, *Agric. Biol. Chem.* 55 (1991) 2629-2631.

[11] R. Fan, S. Ban, X. Feng, C. Zhao, Q. Li, , Synthesis and Anti-VSMC Vegetation Activities of New Aurone Derivatives Chem. Res. Chin. Univ. 28 (2012) 438-442.

[12] A. Ichihara, H. Tazaki, M. Miki, S. Sakamura, Solanapyrones A, B and C, phytotoxic metabolites from the fungus Alternaria solani, Tetrahedron Lett. 48 (1983) 5373-5376.

[13] C. Altomare, G. Perrone, A. C. Zonno, A. Evidente, R. Pengue, R. Fanti, L. Polonelli, Biological Characterization of Fusapyrone and Deoxyfusapyrone, Two Bioactive Secondary Metabolites of Fusarium semitectum, J. Nat. Prod. 63 (2000) 1131-1135.

[14] L. R. Marrison, J. M. Diskinson, I. Fairlamb, J. S, Bioactive 4-substituted-6-methyl-2-pyrones with promising cytotoxicity against A2780 and K562 cell lines, Bioorg Med Chem Lett, 12 (2002) 3509-3513.

[15] O. Talhi, J. A. Fernandes, D. C. G. A. Pinto, F. A. A. Paz, A. M. S. Silva, Diastereoselective synthesis of benzofuran-3(2*H*)-one-hydantoin dyads, Tetrahedron 69 (2013) 5413-5420.

[16] O. Talhi, G. R. Lopes, S. M. Santos, D. C. G. A. Pinto, A. M. S. Silva, Visible light-induced diastereoselective E/Z-photoisomerization equilibrium of the C=C benzofuran-3-one-hydantoin dyad, J. Phys. Org. Chem. 27 (2014) 756-763.

[17] M. CindricVis, N. Vrdoljak, T. Kajfez, P. Novak, A. Brbot-Saranovic, N. Strukan, B. Kamenar, Synthesis and characterization of new dinuclear complexes of molybdenum (V) with β′-hydroxy-β-enaminones, Inorganica Chimica Acta, 328 (2002) 23–32.

[18] M. Massacesi, R. Pinna, G. Ponticelli, G. Puggioni, Platinum(IV) chloride complexes with heterocyclic ligands. J. Inorg. Biochem. 292 (1987) 95–100.

[19] N. Galva'n-Tejadaa, S. Berne'sb, S.E. Castillo-Bluma, H. Nothc, R. Vicented, N. BarbaBehrens, Supramolecular structures of metronidazole and its copper(II), cobalt(II) and zinc(II) coordination compounds , J. Inorg. Biochem. 91 (2002) 339–48.

[20] Z. Travnicek, J. Mikulík, M. Cajan, R. Zboril, I. Popa, Novel iron complexes bearing N6-substituted adenosine derivatives: Synthesis, magnetic, ^{57}Fe Mössbauer, DFT, and in vitro cytotoxicity studies Bioorg. Med. Chem, 16 (2008) 8719–8728.

[21] M. L. McKee, S. M. Kerwin, Synthesis, metal ion binding, and biological evaluation of new anticancer 2-(2'-hydroxyphenyl)benzoxazole analogs of UK-1 ,Bioorg. Med. Chem, 16 (2008) 1775–1783.

[22] J.C.G. Bunzli, The europium (III) ion as spectroscopic probe in bioinorganic chemistryInorg. Chim. Acta, 139 (1987) 219-222.

[23] W. Horrocks, M. Albin, Prog, Lanthanide ion luminescence in coordination chemistry and biochemistry. Prog. In Inorg. Chem. 31 (1984) 1-104.

[24] F.S. Richardson, Terbium(III) and europium(III) ions as luminescent probes and stains for biomolecular systems, Chem. Rev. 82 (1982) 541-552.

[25] C. Bisi Castellani, O. Carugo, Studies on fluorescent lanthanide complexes. New complexes of lanthanides (III) with coumarinic-3-carboxylic acid. Inorg. Chim. Acta 159 (1989) 157-161.

[26] C. Bisi Castellani, O. Carugo, C. Tomba, A. Invernizzi Gamba, Fluorescent lanthanide complexes. 1. Reaction between terbium(3+) and 4-oxo-4H-1-benzopyran-3-carboxaldehyde in alcoholic medium. Inorg. Chem. 27 (1988) 3965-3968.

[27] F. Boschetti, F. Denat, E. Espinosa, A. Tabard, Y. Dory, R. Guilard, Regioselective N-Functionalization of Tetraazacycloalkanes. J. Org. Chem. 70 (2005) 7042-7053.

[28] R.R. Zaky, T.A. Yousef, Spectral, magnetic, thermal, molecular modelling, ESR studies and antimicrobial activity of (E)-3-(2-(2-hydroxybenzylidene) hydrazinyl)-3-oxo-n(thiazole-2-yl)propanamide complexes. J. Mol. Struct. 1002 (2011) 76-85.

[29] A. Onder, M. Turkyilmaz, Y. Baran, Synthesis, spectroscopic, magnetic and thermal properties of copper(II), nickel(II) and iron(II) complexes with some tetradentate ligands: Solvatochromism of iron(II)–L2 Inorg. Chim. Acta. 391 (2012) 28-35.

[30] F. Derridj, K. Si Larbi, J. Roger, S. Djebbar, H. Doucet, Palladium-catalyzed direct arylation using free NH2 substituted thiophene derivatives with inhibition of amination type reaction. Tetrahedron, 68 (2012) 7463-7471.

[31] B. Čobeljić, A. Pevec, I. Turel, M.Swart, D. Mitić, M. Milenković, I. Markovic´, M. Jovanovic´, D. Sladic´, M. Jeremic´, K. elkovic´, Synthesis, characterization, DFT calculations and biological activity of derivatives of 3-acetylpyridine and the zinc(II) complex with the condensation product of 3-acetylpyridine and semicarbazide. Inorg. Chim. Acta 404 (2013) 5-12.

[32] Y. Abdi, B. Boutemeur-Kheddis, M. Hamdi, O. Talhi, F. A. Almeida Paz, G. Kirsch, A. M. S. Silva, A One-Pot Diastereoselective Synthesis of 2-[Aryl(hydroxy) methyl]-6-methyl-2H-furo[3,2-c]pyran-3,4-diones: Crystallographic Evidence for the Furanone Ring Closure, Synlett. 26 (2015) 1749-1753. http://dx.doi.org/10.1055/s-0034-1380214.

[33] M.J. Frisch, G.W. Trucks, H.B. Schlegel, G.E. Scuseria, M.A. Robb, J.R. Cheeseman, J.A. Montgomery Jr., T. Vreven, K.N. Kudin, J.C. Burant, J.M. Millam, S.S. Iyengar, J. Tomasi, V. Barone, B. Mennucci, M. Cossi, G. Scalmani, N. Rega, G.A. Petersson, H. Nakatsuji, M. Hada, M. Ehara, K. Toyota, R. Fukuda, J. Hasegawa, M. Ishida, T. Nakajima, Y. Honda, O. Kitao, H. Nakai, M. Klene, X. Li, J.E. Knox, H.P. Hratchian, J.B. Cross, C. Adamo, J. Jaramillo, R. Gomperts, R.E. Stratmann, O. Yazyev, A.J. Austin,R. Cammi, C. Pomelli, J.W. Ochterski, P.Y. Ayala, K. Morokuma, G.A. Voth, P. Salvador, J.J. Dannenberg, V.G. Zakrzewski, S. Dapprich, A.D. Daniels, M.C. Strain, O. Farkas, D.K. Malick, A.D. Rabuck, K. Raghavachari, J.B. Foresman, J.V. Ortiz, Q. Cui, A.G. Baboul, S. Clifford, J. Cioslowski, B.B. Stefanov, G. Liu, A. Liashenko, P. Piskorz, I. Komaromi, R.L. Martin, D.J. Fox, T. Keith, M.A. Al-Laham, C.Y. Peng, A. Nanayakkara, M. Challacombe, P.M.W. Gill, B. Johnson, W. Chen, M.W. Wong, C. Gonzalez, J.A. Pople, Gaussian 03 Revision C. 01, Gaussian, Inc, Wallingford CT, 2004.

[34] A.D. Becke, Density-functional exchange-energy approximation with correct asymptotic behavior, Phys. Rev. A 38 (1988) 3098-3100.

[35] A.D. Becke, Density-functional thermochemistry. III. The role of exact exchange J. Chem. Phys. 98 (1993) 5648-5652.

[36] A.D. Becke, A new mixing of Hartree–Fock and local density-functional theories, J. Chem. Phys. 98 (1993) 1372-1377.

[37] P.J. Hay, W.R. Wadt, *Ab initio* effective core potentials for molecular calculations. Potentials for K to Au including the outermost core orbitals, J. Chem. Phys. 82 (1985) 299-310.

[38] C. Lee, W. Yang, R.G. Parr, Development of the Colle-Salvetti correlation-energy formula into a functional of the electron density, Phys. Rev. B Condens. Matter 37 (1988) 785-789.

[39] N. Bensouilah, M. Abdaoui, Inclusion complex of N-nitroso, N-(2-chloroethyl), N′, N′-dibenzylsulfamid with β-Cyclodextrin : Fluorescence and molecular modeling; Comptes Rendus Chimie 15 (2012) 1022–1036.

[40] N. Marchal, J. L. Bourdou, Richard C. Les milieux de culture. third ed. France: Applied biology, 1997.

[41] A.L. Barry, S.D. Brown, Fluconazole Disk Diffusion Procedure for Determining Susceptibility of Candida Species, J. Clin. Microbiol. 34 (1996) 2154-2157.

[42] National Committee for Clinical Laboratory Standards, Methods for Dilution Antimicrobial Susceptibility Tests for Bacteria that Grow Aerobically, Approved standard InNCCLS document M7-A4, fourth ed., National Committee for Clinical Laboratory Standards, Wayne, Pa., 1997.

[43] M. Shebl, Saied M.E. Khalil, F.S. Al-Gohani, Preparation, spectral characterization and antimicrobial activity of binary and ternary Fe(III), Co(II), Ni(II), Cu(II), Zn(II), Ce(III) and UO_2(VI) complexes of a thiocarbohydrazone ligand, J. Mol. Struct. 980 (2010) 78–87.

[44] W.J. Geary, The use of conductivity measurements in organic solvents for the characterisation of coordination compounds, Coord. Chem. Rev. 7 (1971) 81–122.

[45] A. Bouchoucha, S. Zaater, S. Bouacida, H. Merazig, S. Djabbar, Synthesis and characterization of new complexes of nickel (II), palladium (II) and platinum(II) with derived sulfonamide ligand: Structure, DFT study, antibacterial and cytotoxicity activities, J. Mol. Struct. 1161 (2018) 345-355.

[46] M. Mohamdi, N. Bensouilah and M. Abdaoui, Investigation of charge transfer complexes formed between (S, S)-bis-N,N-sulfonyl bis-L-phenylalanine dimethylester donor with tetracyanoethylene and chloranil as π acceptors: Experimental and DFT studies, Journal of Theoretical and Computational Chemistry, 15 (2016) 1650009 1-39.

[47] S. Sadaoui-Kacel, S. Zaater, N. Bensouilah, S. Djebbar, Novel repaglinide complexes with manganese (II), iron(III), copper(II) and zinc(II): spectroscopic, DFT characterization and electrochemical behavior, J. Stru. Chem. 57 (2016) 1519-1530

[48] Bouchoucha, A.; Terbouche, A.; Bourouina, A. and S. Djebbar, New complexes of manganese (II), nickel (II) and copper (II) with derived benzoxazole ligands: Synthesis, characterization, DFT, antimicrobial activity, acute and subacute toxicity, Inorg. Chim. Acta., 2014, 418, 187-197.

[49] A.S. Gaballa, A. S. Asker, A. S. Barakat, S. M. Teleb, Synthesis, characterization and biological activity of some platinum(II) complexes with Schiff bases derived from salicylaldehyde, 2-furaldehyde and phenylenediamine, Spectrochim. Acta. A., 67 (2007) 114-121.

[50] S. Belaid, A. Landreau, S. Djebbar, O. Benali-Baitich, G. Bouet, J.P. Bouchara, Synthesis, characterization and antifungal activity of a series of manganese(II) and copper(II) complexes with ligands derived from reduced *N,N′-O*-phenylenebis(salicylideneimine)
J. Inorg. Biochem. 102 (2008) 63-69.

[51] V.T. Kasmov, I. Karatal, F. Koksal, Synthesis and ESR studies of redox reactivity of bis (3,5-di-*tert*-butyl-1,2-benzoquinone-2-monooximato)Cu(II), Spectrochim. Acta Part A, 56 (2000) 841-1034.

[52] M. Kalanithia, M. Rajarajan, P. Tharmaraj, C.D. Sheela, Spectral, biological screening of metal chelates of chalcone based Schiff bases of N-(3-aminopropyl) imidazole, Spectrochim. Acta Part A, 87 (2012) 155-162.

[53] L. Mitu, N. Raman, A. Kriza, N. Stanica, M. Dianu, Template synthesis, characterization and antimicrobial activity of some new complexes with isonicotinoyl hydrazone ligands, J. Serb. Chem. Soc. 74 (2009) 10, 1075-1084.

[54] R. R. Zaky, T.A. Yousef, Spectral, magnetic, thermal, molecular modelling, ESR studies and antimicrobial activity of (*E*)-3-(2-(2-hydroxybenzylidene) hydrazinyl)-3-oxo-*n*(thiazole-2-yl)propanamide complexes, J. Mol. Struct. 2011, 1002, 76-85.

[55] Z. Derikvand, N. Dorosti, F. Hassanzadeh, A. Shokrollahi, Z. Mohammadpour, A. Azadbakht, Three new supramolecular compounds of copper (II), cobalt (II) and zirconium (IV) with pyridine-2, 6-dicarboxylate and 3, 4-diaminopyridine: Solid and solution states studies, Polyhedron, 43 (2012) 140-152.

[56] V. T. Kasumov, F.Köksal, Synthesis, ESR, UV-Visible and reactivity studies of new bis(N-dimethoxyaniline-3,5-(t)Bu2-salicylaldiminato)copper(II) complexes, Spectrochim. Acta A Mol. Biomol. Spectrosc. 98 (2012) 207-214. doi: 10.1016/j.saa.2012.07.122. Epub 2012 Aug 4.

[57] N. Tidjani-Rahmouni, N. H. Bensiradj, S. Djebbar, O. Benali-Baitich, Synthesis, characterization, electrochemical studies and DFT calculations of amino acids ternary complexes of copper (II) with isonitrosoacetophenone. Biological activities, J. Mol. Struct. 1075 (2014) 254–263.

[58] J. Campora, M. A. Cartes, A. Rodriguez-Delgado, A. M. Naz, P. Palma, C. M. Perez, Studies on the atropisomerism of Fe(II) 2,6-bis(N-arylimino)pyridine complexes, Inorg. Chem. 48 (2009) 3679-3691.

[59] Z. Derikvand, N. Dorosti, F. Hassanzadeh, A. Shokrollahi, Z. Mohammadpour, A. Azadbakht, Three new supramolecular compounds of copper (II), cobalt (II) and zirconium (IV) with pyridine-2,6-dicarboxylate and 3,4-diaminopyridine: Solid and solution states studies, Polyhedron, 2012, 43, 140-152.

[60] R. Ramesh, S. Maheswaran, Synthesis, spectra, dioxygen affinity and antifungal activity of Ru(III) Schiff base complexes, J. of Inorg. Biochem. 96 (2003) 457-462.

[61] A. Onder, M. Turkyilmaz, Y. Baran, Synthesis, spectroscopic, magnetic and thermal properties of copper(II), nickel(II) and iron(II) complexes with some tetradentate ligands: Solvatochromism of iron(II)–L2, Inorg. Chim. Acta. 391 (2012) 28-35.

[62] F. Yahia, E. K. Karem, S. A. Hussain, Synthesis, Spectral Characterization and Antimicrobial Activity of Some Transition Metal Complexes with new Schiff Base ligand (BDABI), . Oriental J. of Chem. 34 (2018) 434-443.

[63] R. C. Chikate, A.R. Belapure, S.B. Padhye, D.X. West, Transition metal quinone–thiosemicarbazone complexes 1: Evaluation of EPR covalency parameters and redox properties of pseudo-square-planar copper(II)–naphthoquinone thiosemicarbazones, Polyhedron, 24 (2005) 889-899.

[64] Z. Zhou, R. G. Parr, Activation hardness: new index for describing the orientation of electrophilic aromatic substitution, J. Am. Chem. Soc. 112 (1990) 5720–5724.

[65] R. K. Singh, S. K. Verma, P. D. Sharma, DFT based Study of interaction between Frontier Orbitals of Transition Metal Halides and Thioamides, Int. J. of Chem. Tech. Res. 3 (2011) 1571–1579.

[66] R.G. Pearson, Hard and soft acids and bases: the evolution of a chemical concept. Coord. Chem. Rev. 100 (1990) 403–425.

[67] N. Bensouilah, B. Boutemeur-Kheddis, H. Bensouilah, I. Meddour, M. Abdaoui ; Host-guest complex of nabumetone: β-cyclodextrin: quantum chemical study and QTAIM analysis; J. Incl Phenom Macrocycl Chem, 87 (2017) 191–206

[68] N. Bensouilah, H. Fisli, N. Dhaoui, N. B. Cherif and M. Abdaoui, Solvent effects of N-nitroso, N-(2-chloroethyl), N′,N′-dibenzylsulfamid and its copper(II) and cobalt(II) complexes: fluorescence studiesJ. biol. and chem. lum. 28 (2013) 30–37.

[69] N. Bensouilah, H. Fisli, H. Bensouilah, S. Zaater, M. Abdaoui, B. Boutemeur-Kheddis, Host-guest complex of N-(2-chloroethyl), N-nitroso, N', N'-dicyclohexylsulfamid with β-cyclodextrin: Fluorescence, QTAIM analysis and structure-chemical reactivity, J. Mol. Struct.1146 (2017) 179-190.

[70] A. T. Ardjani, S. M. Mekelleche, Theoretical study of the structure, spectroscopic properties and anti-cancer activity of tetrahydrochromeno[4,3-b]quinolines, J. The Comp. Chem. 14 (2015) 1550052- 1550069.

[71] K. Poole, Multidrug resistance in gram-negative bacteria. Curr Opin Microbiol, Current opinion in microbiology, 4 (2001) 500-508.

[72] R.H. Weiss, D.P. Riley, in: N.P. Farrell (Ed.), Uses of Inorganic Chemistry in Medicine, Royal Society of Chemistry, Cambridge, (1999) 77–92.

[73] J. Borras, G. Alzuet, S. Ferrer, C.T. Supuran, in: C.T. Supuran, A. Scozzafava, J. Conway (Eds.), Carbonic Anhydrase: its Inhibitors and Activators, Metal Complexes of Heterocyclic Sulfonamides as Carbonic Anhydrase Inhibitors, CSC Press, Boca Raton, 2004.

[74] A.S. Chaudhary, R. Singh, Tetraazamacrocyclic Complexes of Tin (II): Synthesis Spectroscopy and Biological screening. Bol. Soc. Quim. 47 (2002) 203-211.

[75] Carmen M. Sharaby, Preparation, characterization and biological activity of Fe(III), Fe(II), Co(II), Ni(II), Cu(II), Zn(II), Cd(II) and UO(2)(II) complexes of new cyclodiphosph(V)azane of sulfaguanidine.Spectrochim. Acta A 62 (2005) 326-334.

[76] V.T. Kasmov, I. Karatal, F. Koksal, Synthesis and ESR studies of redox reactivity of bis (3,5-di-tert-butyl-1,2-benzoquinone-2-monooximato) Cu(II) Spectrochim. Acta A. 56 (2000) 841-850.

[77] B.S. Creaven, B. Duff, D.A. Egan, K. Kavanagh, G. Rosair, V.R. Thangella, M. Walsh, Anticancer and antifungal activity of copper(II) complexes of quinolin-2(1H)-one-derived Schiff bases, Inorg. Chim. Acta. 363 (2010) 4048-4058.

Highlights

The Highlights of research are as follows:

1- Four new metal complex derivatives of two new ligands 2-(hydroxy(phenyl)-6-methyl-2H-furo[3,2-c]pyran-3,4-dione (**L^1**) and 2-(hydroxyl (2-hydroxyphenyl) -6-methyl-2H-furo[3,2-c]pyran-3,4-dione (**L^2**) with the metal ions Mn(II) and Cu(II) have been successfully prepared.

2- The complexes obtained are investigated by: FT-IR, UV-vis, ESR and magnetic measurements.

3- Theoretical calculations invoking geometry optimization and molecular orbital description HOMO and LUMO are done using DFT/LAN2DZ density functional theory.

4- The antimicrobial activity of the ligands and their complexes was evaluated in vitro against different bacteria and fungi.